DEVELOPMENT OF ACTIVATED CARBON FIBERS

FOR ORGANIC REMOVALS

by

Doaa Salim Samhan Alkathiri

A Thesis presented to the Faculty of the
American University of Sharjah
College of Engineering
In Partial Fulfillment
of the Requirements
for the Degree of

Master of Science in
Chemical Engineering

Sharjah, United Arab Emirates

November 2017

© 2017 Doaa Salim Samhan Alkathiri. All rights reserved.

Approval Signatures

We, the undersigned, approve the Master's Thesis of Doaa Salim Samhan Alkathiri.
Thesis Title: Development of Activated Carbon Fibers for Organic Removals.

Signature **Date of Signature** (dd/mm/yyyy)

_____ _____

Dr. Taleb Hassan Ibrahim
Professor, Department of Chemical Engineering
Thesis Advisor

_____ _____

Dr. Yehya Amin El Sayed
Associate Professor, Department of Biology, Chemistry and Environmental Sciences

Thesis Co-Advisor

_____ _____

Dr. Paul Nancarrow
Associate Professor, Department of Chemical Engineering
Thesis Committee Member

_____ _____

Dr. Kazi Fattah
Associate Professor, Department of Civil Engineering
Thesis Committee Member

_____ _____

Dr. Naif Darwish
Head, Department of Chemical Engineering

_____ _____

Dr. Ghaleb Husseini
Associate Dean for Graduate Affairs and Research
College of Engineering

_____ _____

Dr. Richard Schoephoerster
Dean, College of Engineering

_____ _____

Dr. Mohamed El-Tarhuni
Vice Provost for Graduate Studies

Acknowledgement

With happiness and joy, I express praise and gratitude to ALMIGHTY ALLAH who gave me the strength and passion to complete and submit my research work. My deepest sense of appreciation is dedicated to my advisor Dr. Taleb Ibrahim for his continued support, guidance and encouragement throughout my research. I believe that his undoubted trust in me influenced me to work toward my goal in my studies in general and particularly in my thesis research.

I would like to extend my gratitude towards Dr. Yehya Elsayed for his support in my thesis research. This work was enhanced remarkably with his remarks, clear recommendation, discussion and view. He was always willingly present for me and propelled the research forward.

I would like to thank Mr. Nedal Abu-Farah and Mr. Ziad Sara (BCE Department), who were available all the time in the labs and developed my experimental skills. Mr. Ziad trained me to use the TGA and the UV-spectrometer equipment, and Mr. Nedal taught and assisted me to use the Quantachrome machine.

I would like to thank Engineer Mohammed Sabri for his continued help without any hesitation throughout my MSChE studies.

Finally, my deepest gratitude toward my family for their support during my MSChE studies.

Dedication

To my caring Mom and Dad, also to my sister Doha, thank you for all the support you provided.

This work is also dedicated to my supervisors Dr. Taleb Ibrahim and Dr. Yehya El Sayed.

Abstract

Phenols are classified to be one of the most hazardous pollutants found in wastewater. They are discharged into rivers, lakes and seas, causing adverse effects on the enviromental and human health. Adsorption is a well-known technique used to treat wastewater. Activated carbon fibers (ACFs) are highly microporous efficient adsorbents due to their small diameters, high surface area and excellent volumetric capacity. In this work, ACFs were produced using polyacrylonitrile (PAN) fibers using different methods and tools. The fibers were stabilized initially at 250°C followed by carbonization at 850°C at a heating rate of 10°C/min and under the flow of nitrogen gas at a flow rate of 135ml/min. The carbonized fibers were subjected to physical (carbon dioxide) and chemical (potassium hydroxide) activation. The results showed that chemical activation using 3:1 ratio of KOH (wt/wt) produced fibers with a higher surface area of 2885m^2/g compared to the physically activated fibers (774m^2/g). The synthesized ACFs (Syn-ACFs) were compared and characterized in terms of morphology, thermal stability, composition and pore characteristics using SEM, EDS, TGA, CHN and nitrogen isotherm (Quantachrome). Bench scale batch experiments were carried out to determine and compare the adsorption efficiency, optimum parameters and the capacity of Syn-ACF and commercial ACFs (C-ACFs) for p-cresol removal. The adsorption optimum conditions using Syn-ACFs are: Syn-ACFs dosage = 1 g/l, contact time = 30 minutes, temperature = 25°C and initial pH = 4.6. The adsorption study on (Syn-ACFs) gave a higher removal efficiency of 91.0% of p-cresol compared to 71.6% (C-ACFs) at a concentration of 350ppm. In addition, the adsorption isotherms of p-cresol on C-ACFs and Syn-ACFs were found to follow the Langmuir isotherm equation; however, Syn-ACFs revealed a higher adsorption capacity (500mg/g) compared to C-ACFs (294 mg/g) at 25°C. The Syn-ACFs regeneration method was evaluated thermally at elevated temperatures and chemically using ethanol and n-hexane solvents. The thermal regeneration at 600°C achieved a higher removal efficiency of 84% compared to n-hexane (78%). The Syn-ACFs were evaluated for the treatment of produced water to ensure a removal of 71.2%. The results indicated that Syn-ACFs could be used as an efficient adsorbent for p-cresol removal in wastewater.

Keywords: *Activated carbon fibers, Adsorption, Activation, Carbonization, Regeneration, Phenol, Organics, and Wastewater.*

Table of Contents

List of Figures

List of Tables

List of Abbreviations

AC	Activated Carbon
ACFs	Activated Carbon Fibers
COD	Chemical Oxygen Demand
GAC	Granular Activated Carbon
CF	Carbon Fiber
C-ACFs	Commercial Activated Carbon Fibers
Syn-ACFs	Synthesized Activated Carbon Fibers
PAN	Polyacrylonitrile

Chapter 1. Introduction

Chapter 1 provides a brief overview of phenolic compounds present in wastewater and adsorption as a solution to this problem. The objectives of the research are presented along with its contribution. Finally, the thesis structure and organization are defined.

1.1. Overview

Water is essential in our daily lives, and having access to clean water must be one of the primary sustainable development goals that guide humanitarian organizations [1]. According to the United Nations News Center, water in several water supplies and resources is threatened over time due to the insignificant management of water organizations, lack of resource protection, rapid urbanization, climate change and a huge increase in food demand [2]. Moreover, the industrial revolution led to many environmental problems due to the discharge of organic, inorganic, and toxic materials to sewers, rivers, lakes and the sea. The wastewater generated from industrial, domestic and agriculture uses is channeled to return to the environment.

Treating the disposed wastewater allows the environment to receive safe water without causing any danger to human health or nature. Over the years, water pollution has become increasingly rampant and a fundamental problem. Therefore, countries were forced to develop policies and regulation for better control. Produced water is classified to be one of the main waste streams produced as a by-product from oil and gas industries as a mixture of various organic and nonorganic compounds. The effect of discharging produced water to lakes and ocean without treatment is a serious environmental issue all over the world due to further accumulation of waste volume [3]. The discharge of organic pollutants found in produced water lowers the oxygen level in the stream causing a significant negative impact on the living organisms [4]. Therefore, organic pollutants are a concern that requires special treatment and consideration.

Various technologies have been developed specially to remove phenolic compounds for the treatment of organic pollutants present in produced water. However, adsorption is classified to be one of the most efficient and economical methods used in the removal of oil, heavy metals, and organics from produced water. The selection of the appropriate adsorbent is investigated by using various adsorbents such as Granular

Activated Carbon (GAC), Activated Carbon (AC) and Carbon Fibers (CFs). However, activated carbon fibers (ACFs) are more efficient compared to other nano-porous carbon materials. This is due to their small diameters, high surface area and excellent volumetric capacity.

1.2 Thesis Objectives

The focus of this thesis is to develop ACFs of high surface area using PAN fibers; in addition, to optimize the existing methods and tools used in ACFs synthesis. Moreover, evaluate and optimize the removal efficiency of phenolic compounds using the synthesized ACFs (Syn-ACFs) and commercial ACFs (C-ACFs). Furthermore, select the best adsorption isotherm model that describes the removal of phenolic compounds on ACFs. Also, evaluate the removal efficiency of Syn-ACFs to treat produced water. Finally, to develop and evaluate the best regeneration method to regenerate ACFs.

1.3 Thesis Organization

Chapter 2 presents a literature review on phenol, its hazardous effect and the techniques used for treatment. Moreover, a detailed literature review on the importance of ACFs and the methods used to synthesis are also explained. Chapter 3 states all the instrumentations and materials used for the ACFs synthesis. In addition, the adsorption process used for the treatment of phenolic model and produced water were presented. In chapter 4, ACFs synthesis is clarified for different stages with the selection of the best method and tool. Chapter 5 provides the characteristics of C-ACFs and Syn-ACFs using various instrumentations. The adsorption process using C-ACFs and Syn-ACFs was explained in Chapters 6. Finally, Chapter 7 provides a full summary and a conclusion of the research work with recommendations for future work.

Chapter 2. Literature Review

Chapter 2 provides a complete literature review of the common techniques used to treat phenols; in addition, to the importance of adsorption in phenol treatment. A description of the isotherm is presented along with the kinetics models. Finally, the uniqueness of ACFs is explained with a complete review of its synthesis.

2.1. Phenols in Wastewater

Phenolic compounds are present in most of the wastewater generated from pharmaceutical, petrochemical, petroleum, and paper mill industries [5, 6]. According to the USA Environmental Protection Agency (EPA), phenolic compounds are ranked as high-priority pollutants [7]. The presence of phenols or phenolic compounds in small concentration disposed to public sewage, rivers, sea or surface water can cause severe adverse effects to aquatic animals and humans in the short and long term. Discharging the phenolic compounds with other metallic ions may result in complex compounds, which are more carcinogenic than phenolic compounds themselves [8]. Drinking water containing phenol may inflict harmful effects on health including sour mouth, impaired vision and excretion of dark urine. The repeated exposure to phenol through the skin or heated vapor could cause nausea, headache, dizziness, vomiting and even death [9]. Phenolic compounds do not build up in fish and other aquatic animals but becomes toxic when present in concentrations of 9-25mg/l [10]. The presence of phenol and phenolic compounds has increased in industrial wastewater treatment, causing governments to pressure industries to reduce the concentration to be less than 1 mg/l according to EPA standard [11]. The typical effluent concentration of phenolic compounds is found to be 6.8wt% and it can only be safe for release to the environment when the concentration is reduced to 39 parts per billion (ppb) [12].

Table 1: Types of pollutant according to the industrial sector [6].

Sector	**Pollutant**
Iron and steel	Oil, metals, acids, phenols, and cyanide
Textiles and leather	Solids , sulfates and chromium
Pulp and paper	Solids , Chlorinated organic compounds
Petrochemicals and refineries	mineral oils, phenols and chromium
Chemicals	Organic chemicals, heavy metals, and cyanide
Non-ferrous metals	Fluorine
Microelectronics	Organic chemicals

Mining	Metals, acids and salts

Table 1 shows a general division of pollutant in various industrial sectors. In general types of industrial wastewater could be classified, based on the source, into inorganic and organic wastewaters.

The removal of phenolic compounds pollutant from water could be done through three conventional methods: physical, chemical and biological treatment [13, 14, 15, 16]. The physical method involves adsorption which is known to be the best low-cost, effective and most frequently used method. Alternatively, the chemical method is based on extraction where carbon dioxide and water are used in an extractor to remove all the phenol from the water [17]. The phenol is removed as gas; clean water is discharged, and carbon dioxide is recycled. Furthermore, electrochemical incineration is a method that involves using boron-doped diamond electrodes to mineralize the phenolic compounds in wastewater. In addition, an important low cost chemical technique is wet air oxidation, which is highly usable when the concentration of phenol is low and biological treatment isn't feasible. It involves partially oxidizing the material into biodegradable components using oxygen and carbon dioxide [18]. The biological process, which is classified into microbial degradation and aerobic biodegradation. Aerobic biodegradation is the most common biological method in phenolic compounds removal [19]. The biological treatment is known to be efficient and economical. However, it's difficult for removing phenolic compounds at lower concentration than 200 mg/l or at high phenol concentrations since it prevents the growth of microorganisms. The existence of phenol as a toxic pollutants results in the deflocculation that cause settling problems in the clarifier [20].

Table 2: Common techniques for the treatment of phenols.

Method	**Features**	Ref
Polymerization	• 90% removal efficiency • Not efficient with high phenol concentration	[21] [22]
Electro Coagulation	• 97% removal efficiency • Not efficient with high phenol concentration	[23] [24]
Extraction	• Good separation effect and low energy consumption • 70% removal efficiency	
Photocatalytic Degradation	• Effective in the removal of phenol up to 92.4%	[25] [26]

	• Not efficient 0.2mg/ml	
Biological methods	• Efficient and economical • 75% removal efficiency	[27] [28]
Electron-Fenton method	• Economical • Short reaction time • No energy input • Formation of ferric hydroxide as sludge	[29]
Membrane based separation	• Lower energy consumption • High quality effluent	
Catalytic wet oxidation process	• Efficient in the removal of phenol • High cost	
Adsorption	• 98% Removal efficiency • Treat high phenol concentration • Feasible & economical	[30]

Table 2 summarizes the common techniques used to treat phenols with the advantages and disadvantages of each technique. Concluding that the adsorption technique would be the best selection for the treatment of phenolic compounds in wastewater treatment. However, various adsorbents were used to treat pollutants presented in water such as: zeolites, activated carbon (granular, powder, etc.), activated alumina, silica gel, luffa cylindrica fibers, sawdust, rice straw and activated carbon fibers.

2.2. Adsorption

The adsorption process is explained by the adhesion of molecules, gas, liquid, or solid to a given surface. Adsorption occurs mainly due to the unbalanced residual forces in the level of solute in the solution. This causes the residual forces to continue the sticking of the gas, liquid, or solid molecules on the surface with which it comes into contact. The adsorption continues until the level of solute remaining in the solution is in equilibrium with the adsorbate on the given surface [31]. The adsorbate entails the molecules of the substance sticking on the given surface while the adsorbent entails the substance on the surface that perpetrates the adsorption process. The most preferred adsorbent are activated carbon fibers (ACFs) in comparison with GAC.

2.2.1. Adsorption application. A common application of the adsorption process is in wastewater treatment, in the removal of organic and inorganic pollutants from the wastewater. However, several applications take place such as [32]:

1) Production of high vacuum

2) Removing coloring substance from solution

3) Heterogeneous catalysis

4) Inert gas separation

5) Silica gel and alumina for desiccation or dehumidification

2.2.2. Adsorption using ACFs. The most remarkable adsorption features of ACF are their large surface area, small and uniform pores. During the activation process in the synthesis of ACFs the porous structure is built in the pyrolyzed residue due to the oxidizing gas.

The pores that are formed could either be formed by the oxidation of layer segments from stacks of graphitic planes or formed by the cracking, removal or cyclization of the less stable groups. When comparing adsorption efficiency in ACF, it is apparent that adsorption is at its best in micropores due to the near distance of the pore walls causing high performance of intermolecular forces [33].

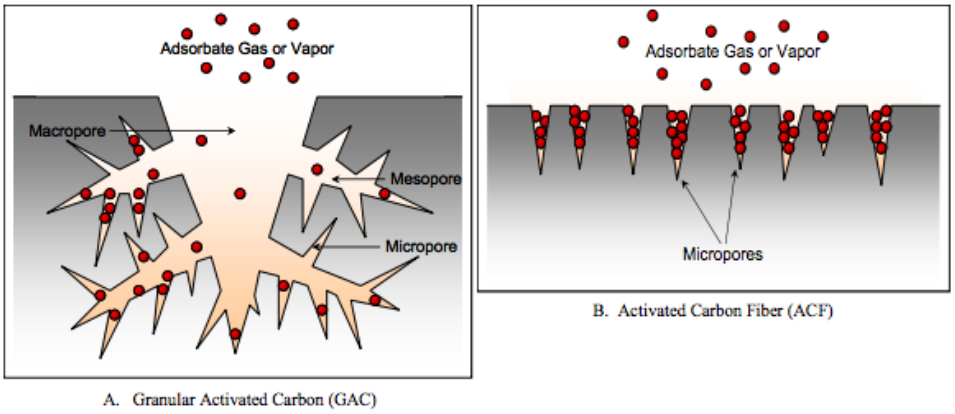

Figure 1: GAC and ACF [33].

Figure 1, part A demonstrates that in GAC, macropores are exposed to the particle external surface, and turn into mespores then micropores. On the other hand, Figure 1B shows that in ACF, the access to micropores is from the outer surface causing a faster adsorption kinetic than GAC. Furthermore, the overlying of forces of adjacent walls in micropores causes their pores to be occupied at low concentrations and is accountable to the adsorption at low VOC concentrations in ambient air conditions.

2.2.3. Adsorption isotherm.

2.2.3.1. Langmuir isotherm. The Langmuir adsorption model analyses show the monolayer adsorption occurs by which the process appears on the sorbent

surface that has the active sites. However, the adsorption process will stop when the active site is totally covered by the sorbent

The Langmuir Model is given as:

$$q_e = \frac{q_m k C_e}{1+kC_e} \quad (3)$$

Where,

C_e= Equilibrium concentration (mg/L),

q_e= Amount of the substance adsorbed at equilibrium per amount of the adsorbent (mg/g),

q_m= Saturation monolayer adsorption capacity (mg/g),

k = Equilibrium adsorption constant (l/mg),

Table 3: Essential characteristics of Langmuir isotherm [34].

Value of R_L	Type of isotherm
$R_L > 1$	Unfavorable
$R_L = 1$	Linear
$0 < R_L < 1$	Favorable
$R_L < 1$	Irreversible

Table 3 shows the main features of Langmuir isotherm that can classify the type of isotherm depending on the separation factor R_L value, which is calculated using the following equation:

$$R_L = \frac{1}{1+bC_i} \quad (4)$$

Where,

R_L is the separation factor that determines whether the adsorption process is favorable or not, b is the Langmuir constant ($\frac{L}{mg}$), and c_i is the initial concentration of adsorbate ($\frac{mg}{L}$) [31].

2.2.3.2. Freundlich isotherm. The Freundlich model is considered to be one of the most elementary models. In addition, it's an empirical expression that is designed to explain the heterogeneous surface.

The Freundlich adsorption model is given as [35]:

$$q_e = k_f C_e^{\frac{1}{n}} \quad (5)$$

Where,

q_e is the amount of the substance adsorbed at equilibrium per amount of the adsorbent (mg/g), K_F is the adsorption capacity of multilayer ($\frac{m^{(1-\frac{1}{n})} L^{\frac{1}{n}}}{g}$), C_e is the equilibrium concentration (mg/L) and n is Freundlich constant associated to the adsorption intensity.

2.2.3.3. Temkin isotherm. In acidic solution, the Temkin equation was primarily suggested to report the adsorption capacities of hydrogen on platinum electrodes. The function of temperature in the Temkin isotherm during the derivation is linear, not logarithmic as in the Freundlich expression.

The linear form of the Temkin expression:

$$q_e = B\log k_t + B\log C_e \quad (6)$$

Where,

q_e is the amount of adsorbed oil per unit mass of adsorbent ($\frac{mg}{g}$), b is Temkin constant related to heat adsorption ($\frac{J}{mole}$) , $B = \frac{RT}{b}$, K_t is the Temkin constant ($\frac{L}{mg}$), T is the total temperature (K), R is the gas constant , $\frac{1}{b}$ is the absorption potential of the adsorbent.

2.2.3.4. Dubinin-Radushkevich adsorption isotherm. The energy of sorption and mechanism are classified using The Dubinin-Radushkevich model (D-R). Moreover, the (D-R) model differentiates between chemisorption and physisorption to give outstanding results of equilibrium data in the gas phase.

The Dubinin-Radushkevich (D-R) model is expressed mathematically as:

$$q = q_e \exp(-B_D \left(RT\ln\left(1 + \frac{1}{C_e}\right)\right)^2 \quad (7)$$

Where,

q_e= Equilibrium adsorption capacity ($\frac{mg}{g}$),

B_D=Free energy of adsorption per mole of adsorbate,

C_e= Equilibrium concentration ($\frac{mg}{L}$),

T = Total temperature (K),

R = Gas constant.

2.2.4. Adsorption kinetics. Kinetic adsorption is analyzed to estimate the limitations of adsorption such as retention of adsorbent, optimum contact time, and adsorption kinetics. To achieve equilibrium, the kinetic study develops some data about the pathway and time that depends on how the material performs and on the inherent characteristics. However, some of the operating parameters of the process may also affect kinetics [36]. In this study, the most common models that are used to test the adsorption kinetics are pseudo-first- and second-order kinetic.

2.2.4.1. Pseudo first order model. The pseudo first order model (Lagergen Model), describes the adsorption at the interface of liquid and solid. This example is as follows:

$$\frac{dq}{dt} = k_1(q_e - q_t) \tag{8}$$

The linear form is:

$$\ln(q_e - q_t) = \ln q_e - K_1 t \tag{9}$$

Where,

q_t is the amount of lead ions removed at time t ($\frac{mg}{g}$), q_e is the capacity of adsorption at equilibrium($\frac{mg}{g}$), K_1 is the pseudo-first-order rate constant($\frac{1}{min}$), t is the contact time (min).

Plot a graph between $\ln(q_e - q_t)$ vs t to get the rate constant K_1 value. The plotting forms a linear curve equation in which k_1 is given from the slope [36, 37].

2.2.4.2. Pseudo second-order model. Second order rate equation is given by:

$$\frac{dq}{dt} = k_2(q_e - q_t)^2 \tag{10}$$

Rearranging the equation gives us the following linear form:

$$\frac{t}{q_t} = \frac{1}{k_2 q_e{}^2} + \frac{t}{q_e} \tag{11}$$

Where,

q_e is the adsorption capacity at equilibrium ($\frac{mg}{g}$), q_t is the instantaneous adsorption capacity ($\frac{mg}{g}$), T is time (min), k_1 is the rate constant of the pseudo first order reaction($\frac{1}{min}$) and k_2 is the rate constant for the pseudo second order reaction ($\frac{1}{min\,g}$). k_1 is calculated from the slope, k_2 is the y-intercept of ($\frac{1}{{q_e}^2}$) of the graph plot between $\frac{t}{q_t}$ and t [37].

2.3. Activated carbon fibers (ACFs)

In 1960's activated carbon fibers were initially produced for resistance textiles. Later, industries drove the technology toward production of high-modulus as strength fibers. In 1963, the Carborundum Company prepared cross-linked phenol fibers that could be made by spinning from a Novalic melt, and subsequently cured it with hydrochloric acid (HCI) and formaldehyde (CH_2O). The fiber produced by the process is used in textile forms [38]. In 1968 Kynol is heated in steam with a range at 700-900°C to produce high surface area of ACFs. In the early 1990s, a program was initiated at the University of Illinois to help develop a better understanding on the nature of ACFs and focused their research toward development of ACFs at a cost competitive to GACs. They succeeded in modifying the pore surface chemistry of ACFs allowing their use for specific applications. For instance, the pore surface chemistry has been tailored to be acidic or basic, neutral or polar according to the adsorption application. Activated carbon fibers (ACFs) can be made from several precursors such as: polyacrylonitrile (PAN), coal, rayon, phenolic resins and pitches [39]. Using different precursors will modify the properties and define pore texture of the ACFs [40]. Due to their high adsorption performance and greater strength, the PAN and Pitch based ACFs have gained much attention of many researchers in comparison with other precursors [41]. ACFs from a Pitch-based carbon precursor proved a high adsorption capacity for toluene [42]. In addition, another research highlighted the removal of sulfur oxide (SO_x) and nitrogen oxide (NO_x) using different ACFs precursors to compare between their removal efficiencies. The research showed that Pitch-based ACFs achieved higher SO_x in comparison with other ACF precursors; however, ammonia (NH_4) used with ACF gave an effective removal of NO_x [43]. On the other hand, ACF's synthesized using

PAN precursor achieved unique adsorption capability and outstanding strength in many research papers [44, 45, 46, 47].

2.3.1. ACFs precursors. In chemistry, precursors are defined to be compounds that contribute in the production of another compound within a chemical reaction. Four types of precursors' materials are used to produce ACFs: Phenolic resins, PAN, pitch, and cellulosic precursors [48]. The precursors undergo pyrolysis followed by an additional activation process to produce ACFs. Both the nature of precursor and the method of activation have strong influences on the adsorption capacity with the porous structure. Adsorption in the pores is driven by the effect of the dispersion component of the vander walls forces [39].

2.3.1.1. Phenolic resins precursors. Phenol-formaldehyde resins (Phenolic resins) are produced from the reaction of formaldehyde-substituted phenol or phenol reactions. Phenolic resins are applied in the production of circuit boards and in molded production billiard balls. ACFs using phenolic resin precursors are developed by carbonization within a temperature of 600 ^{0}C followed by activation using carbon dioxide (>850 ^{0}C) or steam (>700 ^{0}C) [49]. Kleeberg made the first true phenol-formaldehyde resin in the 1891 [50]. They are stiff, strong, resistant to flame, easy in processing, less toxic and more economical. In addition to carbonation, phenolic resin can be formulated for properties enhancement with excellent resistance from acids, organic solvents, and water. The production of activated carbon fibers was investigated by different researchers and published in many books and articles using phenolic resins [39, 51, 52].

2.3.1.2. Pitch precursors. Pitch precursors that are used to produce activated carbon fibers contain 80% carbon. It is a residue produced from a petroleum and coal tar operation in refinery, and is described to be a high molecular weight. To form the carbon fiber, the raw material must be converted from an isotropic material to an anisotropic material. Uniform structures made of isotropic materials block the light from passing in all direction; in contrast, anisotropic materials allow light to pass through them [53]. The conversion requires a temperature range between 400-500°C under an inert atmosphere or vacuum. The production of carbon fibers using Pitch precursors requires three main steps: melt-spinning, oxidation (stabilization), carbonization and activation. The fibers are produced through the melt-spinning of

pitch precursors. The stabilization, or in other words called oxidation, is performed to improve the mechanical properties and avoid the deformation of the fiber in the carbonization process [39]. The carbonization could either be through an inert environment with nitrogen (N_2) or with argon gas with a temperature less than 1600°C.

2.3.1.3. Polyacrylonitrile precursors (PAN). PAN is the dominant precursor among other precursors in the production of ACFs. PAN is a repeated unit of nitrile groups with respect to a polymer as a backbone. The structure is extended due to the nitrile group high electronegativity [39]. The process of manufacturing carbon fibers using PAN precursors is done through several steps: polymerization of PAN-based precursors, fibers spinning (wet spinning), thermal stabilization, carbonization, graphitization and activation [49]. PAN is polymerized by radical polymerization using acrylonitrile with a specific comonomer content. The use of comonomers recovers the mechanical and processability process of the PAN fiber. In addition, they improve the molecular orientation in the final produced carbon fiber and ease the stabilization during the cyclization reaction. [54]. Vinyl esters are used as comonomers resulting in an improvement in the solubility of the polymer in the spinning solvent (wet spinning). Carboxylic acid is another active comonomers that increases the carbon yield and favors oxidation. The confirmed effective acids are: itaconic acid>methacrylic acid>acrylic acid> acrylamide [55]. In fact, PAN precursors contribute to 90% of the total production of carbon fibers (CFs). PAN is stronger than other precursors since it provides high carbon yield and requires high melting point [39].

2.3.1.4. Biomass raw materials. In addition to the listed precursors and carbon sources, agriculture wastes are also used as raw materials to prepare ACFs. They are classified as biomass to produce carbon-neutral natural fibers. They include wood [56, 57], coconut fibers [58], oil palm fibers [59], bamboo fibers [60, 61], flax [62]and many other agriculture by-products. The agriculture by-products showed a good adsorption capacity; however, the application and preparation are still limited in comparison with commercial synthetic ACFS [39]. The precursors are preferred than biomass in the production of ACFs since they are easy to converge and produce higher carbon yield [54].

2.3.2. Synthesis of ACFs using polymeric fibers. The synthesis of precursors depends on the type of precursors; however, polymeric ACF commonly uses similar

synthesis process [54]. The polymeric fiber precursor undergoes four main steps, stabilization, carbonization, activation and chemical modification.

2.3.2.1. Stabilization. Stabilization is the main stage in the preparation of the fiber precursor. The stabilization protects the shape of the fiber, preventing them from melting and sticking together. The completion of this stage avoids excessive volatilization of carbon elements and maximizes the precursor fiber carbon yield [54]. Cyclization of the nitrile groups (C=N) occurs in the stabilization process to develop a chain of –C=N-C=N-, by which the triple bound of the nitrile group converts to double bond with a bond to a carbon atom [63].

Temperature, oxygen concentration and the chemical nature parameter affect the rate of stabilization [64]. According to different studies the optimal heat treatment temperature varies from one study to another. However, the stabilization process temperature is usually carried out with a range of 180-300°C [65]. As temperature sets out to be higher than 180°C, the molecular chain moves around and unfolds [54]. On the other hand, studies have different point of view regarding the starting temperature of 180°C, stating that the stabilization fiber temperature is between 200-300°C [66]. Yet, other researchers found that the temperature must be higher than 300°C to achieve complete stabilization process [67, 68]. Thus, the temperature range must not be too high to avoid fuse or burn of the fiber and not too low temperature resulting in a slow reaction or incomplete stabilization process [54]. Oxygen (O_2) acts as an oxidizing agent in the stabilization process, producing oxygen-containing groups through direct oxidation such as: hydroxides (OH), Carbon Dioxides (CO_2), and Carbon Monoxides (CO). Air is the most commonly used oxidizing agent, by which oxygen reacts exothermally with carbon fibers. Using inert is another alternative to air; however, using oxygen with a polymer backbone provides a better stability to withstand the second synthesis stage (carbonization) elevated temperatures [66]. Another study carried out by Fitzer and Muller (1975) indicated that the use of O_2 rather than a gas inert increases the activation energy allowing the formation of an activated center for cyclization [56].

2.3.2.2. Carbonization process. In carbonization process the stabilized fibers are converted to carbon fibers by the removal of noncarbon elements as volatile gases with an inert under a temperature of 800-3000°C [69]. The chemical and physical

properties are changed in this stage. The noncarbon elements recorded to be 50% of the weight of fiber in form of volatiles such as methane, hydrogen, nitrogen, water, carbon dioxide, ammonia and carbon monoxide. The removal of noncarbon elements results in a reduction of the fiber diameter [70]. The temperature of carbonization results in different carbon types. Carbonization under 1000°C temperature produces carbon fibers with low modules in comparison with carbonization under 1500°C which produces intermediate fibers. A study has been done by varying the temperature on the carbonization process of PAN fibers to determine the effect of the ACFs properties. The experiment used nitrogen as an inert along with two temperatures 800°C and 1000°C for 10-90 minutes. Dealing with 800 °C temperature showed an effective increase in the surface area from 500 to 1100 m^2/g and an ACF carbon content increased from 37% to 75%. In addition to that, the binding strength decreased from 3.6 to 1.8 MPa. On the other hand, dealing with 1000°C resulted in a values two times smaller than the ones carbonized under 800°C [71]. Additionally, the temperature effect is studied in another article done by Bin, Feng, Gao-pingm and Yu-sheng to test the properties of the ACFs with a carbonization temperature between 400-900°C. The research paper concluded that there is a relationship between the carbonization temperature and the ACFs microstructure. However, the moderate temperature of the ACFs produced using PAN precursor is found to be 600°C to provide a high surface area with large pore size and volume [72]. Within the selection of temperatures, the inert gas selected to be non-oxidizing media such as: nitrogen, argon or boron tribromide (BBr_3) [47]. The inert is essential in carbonization process to avoid high temperatures during the process. The commonly used inert in most of ACFs synthesis process is nitrogen [72, 17, 71].

2.3.2.3. Activation. Activation energy can be defined as the least amount of energy needed to excite molecules or atoms to a state where they can undergo chemical reaction. Activation is used in removing disorganized carbon that blocks pores in activated carbon fibers and in enlarging the pores diameter [73]. Among the benefits of activation is the ability to model into various shapes, larger capacity, and high speed in performing adsorption and desorption. Activation could be done using two methods: physical activation and chemical activation.

2.3.2.3.1. Physical activation. ACFs preparation by physical activation involves the initial carbonaceous carbon dioxide. The temperature of the selected agent must be between the ranges of 800°C to 1000°C. In the activation process the reaction takes place in the fibers to provide higher pore size for higher removal in adsorption process [74]. Steam and carbon dioxide are the most common activating agents in which carbon reactions are endotherm. CO_2 is helpful in controlling the process of activation because of the slow reaction rate at around 800°C. The mechanism is achieved via gasification reaction using CO_2 as the activating agent. The main reactions can be shown as follows:

$$C + CO_2 => 2CO \quad (12)$$

$$C + H_2O = >CO + H_2 \quad (13)$$

When carbon dioxide is used as the activation agent, it gives out carbon monoxide due to the reaction of free carbons with carbon dioxide. Nevertheless, during the reaction CO_2 with carbon atoms causes chemisorption's of oxygen atom to occur. The oxygen atom chemisorbed forms a surface oxygen complex on the carbon surface. These complexes act as reaction intermediates to produce free CO gas or act as inhibitors for activation reaction throughout blocking the reactive sites [47]. Steam can also be used in physical activation carbon fibers. Nitrogen is normally used in steam activation by which water reacts with carbon quickly and convert it to gas faster at a moderate temperature of 750°C.

2.3.2.3.2. Chemical activation/ modification. Chemical activation refers to the treatment of new materials with activating agents like phosphoric acid, sulphuric acid, zinc chloride, potassium hydroxide, and sodium hydroxide, among others. The combination of activating agents and raw materials produces heat treated under an atmospheric range of between 400°C and 700 °C. After cooling the activated carbon fiber they must be washed with water to remove the chemical traces. In fact, almost all activation agents are agents of dehydration that inhibit tar formation as well as other by-products, such as methanol and acetic acid [73]. Chemical reaction help to increase above 30wt% of carbon yield compared to thermal activation. In the chemical reaction, the increase of activated carbon yield is as a result of acid activation, which promotes redistribution and dehydration of biopolymers. In chemical activation the aliphatic to aromatic conversion takes place. The ratio of impregnation between the mass of raw

material and the activating agent influences the porosity and the carbon yield. Impregnation range of between 0.3 and 3 are in accordance with numerous studies most commonly applied on raw materials. As the ratio of impregnation increases, carbon yield decreases. When a larger amount of acid is applied, an aggressive chemical reaction leads to more organic matter vaporization [39]. According to Nahil (2012) and Molina (1995), a higher impregnation ratio brings about a larger pore size on the final product. Nahil reports that the ratio of activation in chemical reaction affects the polymeric species length. At lower impregnation ratios, the polymeric species length may be small for the creation of narrower pores in microspore range. When higher ratios of impregnation are applied, the length of polymeric species increases, resulting in a wider porosity in the mesopore range. Chemical activation appears more advantageous than the physical activation. This is because of one stage heating, high micro-porous nature, and the high product yield. Chemical activation is, therefore, more suitable for materials yielding higher ash content [75]. In addition, chemical activation helps lower activation temperature, requires a shorter time for activation, and improves the inner porosity development. The use of ACFs in removals might not reach the purity required by law for wastewater treatment. Therefore, producing the ACFs surface must be chemically modified to give effective results in adsorption. The applications of ACFs are conditioned to the chemistry of the surface and heteroatoms content including Nitrogen, oxygen and hydrogen, which influence the properties to give acidic or basic characteristic [76]. To increase the chemical composition of the ACFs, they must be impregnated with chemicals that allow adsorption with reaction of the substance into carbon or with chemicals that act as a catalyst to promote oxidation or transformation [77]. In a recent research paper 2015, the test was done using different chemical modification to test their effect on the adsorption of phenolic compounds [78]. In the paper, two commercial ACFs were used with two chemical aqueous solutions phosphoric acid (H_3PO_4) and potassium hydroxide (KOH) are tested under moderate temperature. The observation of the test was that H_3PO_4 increased the adsorption in comparison with KOH.

2.3.2.4. Characterization. The pore range size is essential in determining the adsorption characteristics effects as established in the isotherm. The pores might vary in shape and size within a given adsorbents. The width of the pore represents the cylindrical pore diameter or the slit-shaped pore distance to the sides. According to the

International Union of Pure and Applied Chemistry (IUPAC), the classifications of pores are shown as summarized as the following:

Table 4: Pore classification in accordance to the pore width size [25].

Pore classification	Pore Width, Å(0.1nm)
Micropores	Less than~20 (2)
Mesopores	Between 20~ and 500 (2-50)
Macropores	More than ~500 (50)

As shown in table 4, the pore classification is linked to the pore width size by which each classification affects adsorption isotherm. For instance, in micropores the pore walls are close to each other, which make interaction potential, larger than wider pores. The gas molecule in the adsorbent interaction energy could be optimized by the intersection of potential fields from adjacent walls. In addition, results show that pores could be filled at low pressures due to the strong interaction. However, it is difficult to map out the isotherm in macropore because the pores are large causing the adsorbate relative pressure (p/p0) near unity. Moreover, the micropores and mesopores are joined by macropores. Micropores are uniform and straight which compose the porous characteristic of ACF, while GAC has macropores, mesopores, and micropores [42]. The characterization could be studied physically or chemically using different instrumentations such as SEM, EDS and TGA.

Chapter 3. Experimental and Methodology

3.1. Materials

PAN fibers were obtained from DFL Minmet Refractories Corp Company in China. Commercial ACFs (C-ACFs) were obtained (C-ACFs) from Anshan Sinocarb Carbon Fibers Co., Ltd in China. P-cresol (Sigma Aldrich, Italy) was used to prepare the model phenol. Potassium hydroxide pellets (KOH) (Emsure, Germany) were used in chemical activation. The pH adjustments were carried out using sodium hydroxide (NaOH) and hydrochloric acid (HCl). Ethanol and n-hexane were used in solvent extraction for regeneration. Surfactant (ENDCOR OCC9783), heavy crude oil (having API < 22.3^{o}) and n-hexane (purity > 95%) were obtained from General Electric UAE, ADNOC UAE, and J.T. Baker (Netherlands).

3.2. Instrumentation

Furnace YKY (Model: CY-M1200-V, USA) used to stabilize the fibers, High temperature tube furnace (Model: OTF-1200x, USA) was used to carbonize and activate the fibers. UV-VIS spectrophotometer (Model: DR-5000, HACH, USA) at a wavelength of 278.0 nm was used to measure the initial and final concentration of p-cresol presented in water. pH meter (Model: 3320, JENNWAY Ltd., UK) and a hot plate stirrer (Model: MSH-20D, DAIHAN Scientific Co. Ltd., Korea) were used to adjust the pH and for stirring and temperature control. Scanning Electron Microscope (SEM), Energy Dispersive X-ray Spectroscopy (EDS) and Thermogravimetric Analyzer (TGA, 4000) (Model: CT06484-4794, Perkin Elmer, USA) were used under a flow of nitrogen with a controlled rate to obtain thermal profile and characterize the samples. Quantachrome (Model: ASIQM0VJ010-4, USA) was used to measure the surface area and pore size distribution of the C-ACFs and Syn-ACFs. CHN elemental analyzer (Model: EA300, Eurovector, Italy) used to determine the carbon, nitrogen and hydrogen content.

3.3. Methods

3.3.1. ACF's synthesis. The ACFs were prepared through three main stages, known as stabilization, carbonization and activation. In each stage, specific procedures were developed to enhance the efficiency of the ACFs development method. In each stage, the ACFs characteristics were determined using TGA, SEM, EDS and CHN which were used to select the best procedure prior to proceeding to the next stage. The

samples of the final stage (activation) were characterized using SEM, EDS, TGA and sorption of nitrogen to assure the presence of optimum structure, surface area, carbon yield, and pore size distribution in the ACFs produced.

3.3.1.1. Stabilization. Stabilization of ACFs is an essential stage to assure that the fibers will not stick together or lose their shape. The PAN fibers were stabilized in the 200-400°C temperature range [65]. About 5-6 grams of PAN fibers were placed in a ceramic crucible inside the furnace. The stabilization temperature of PAN fibers was examined at three different temperatures 200, 250 and 300ºC in the presence of air within the oven environment. The stabilization time was fixed for the three temperatures within 6-7 hours at a rate of 10ºC/min. The fibers were regularly stirred inside the furnace as soon as the temperature reach 100°C to prevent burning and assure homogenous stabilization. The color of fibers was observed during the stabilization on each trial along with the structure of the fibers. Finally, the fibers at three different temperatures were characterized using SEM, EDS, and TGA to verify the stabilization optimum parameters before moving to the carbonization process.

3.3.1.2. Carbonization. In the carbonization process, the stabilized fibers were converted to carbon fibers. The fibers were placed in a quartz boat in the middle of a quartz tube inside the furnace using a metallic hook. The carbonization was done using N_2 gas at a fixed flow rate of 135 ml/min. The carbonization temperatures were varied where the initial temperature was raised from room temperature up to 700, 800, 850 and 950°C using the heating rates of 10°C/min for 1 and 2 hours. The furnace was cooled down before they were removed from the tube. The fibers were characterized using SEM, EDS and TGA.

3.3.1.3. Activation. In the activation process, both physical and chemical activation were examined to determine the best method to obtain the highest surface area, highest carbon yield, improve the porosity and keep the physical strength of ACFs. The physical activation was done using CO_2 at two different temperatures, 850°C and 950°C, as well as varying the flow rate at 135ml/min and 250ml/min. The carbonized fibers were placed in a quartz boat in the middle of a tube furnace with a constant heating rate of 10°C/min for 2 hours. The ACFs were removed when the furnace cooled down. The synthesized ACFs were characterized using SEM, EDS, TGA and the surface area was analyzed.

The chemical activation method was accomplished using KOH pellets mixed with deionized water. ACFs were immersed in KOH slurry and placed in a quartz tube. Three different mass ratios of KOH were examined 3:1, 2:1 and 1:1 (wt/wt). The carbonized fibers were heated at 10^{o}C/min to 950°C at which the temperature was held constant for 1 hour under nitrogen flow rate of 250ml/min. The ACFs were cooled and the excess of KOH was removed using 0.1M of HCl followed by excessive washing with deionized until a pH of approximately 6 was reached. The ACFs were characterized using SEM, EDS, TGA and sorption of nitrogen. The best ratio was selected and the results were confirmed through three replicates to assure reproducibility.

3.3.2. Syn-ACFs structural characterization.

The characterization of PAN fibers and its derivative (stabilized, carbonized and activated) were carried in terms of their pore structure, morphology, elemental composition and thermal stability.

3.3.2.1. SEM/EDS elemental analysis. Scanning Electron Microscope (SEM) produced magnified images using a beam of high energy electrons on the surface of ACFs. The images were used to verify the structural morphology of the fibers at various stages of development. The fibers were placed in a metallic disk and gold coated with a thin layer to reduce the charges for a better image view. The chamber was under a vacuum pressure of $9.0*10^{-4}$ Torr and the electronic beam was in voltage of 15 keV to get the images. Energy Dispersive X-ray Spectroscopy (EDS) was used to determine the chemical composition of the ACFs. The preparation of the ACFs was done without a gold coating film to determine surface chemical composition.

3.3.2.2. Sorption of nitrogen. Nitrogen isotherms were found at a temperature of -195°C. Before, BET- surface area analysis, the samples were kept for 24 hours in the oven at a temperature of 100°C to ensure that there is no moisture content. A mass between 0.04-0.06g ACFs was used for surface area analysis and pore size distribution. The ACFs were placed 16 hours for degassing at a temperature of 120°C prior to analysis. ACFs were cooled down in the degassing station and the weight measurement was taken again after degassing. Brunauer-Emmett-Teller (BET) method was used to calculate ACFs surface area. The Density Functional Theory (DFT) calculates the

surface structure parameters such as specific surface area S_{N2}, volume of micropore V_{mic}, and total volume V_t ACFs [79].

3.3.2.3. CHN elemental analyzer. The analyser is capable of determining the organic matrices content of carbon, hydrogen, nitrogen presented in the sample. The analyzer could be used for various sample types such as, liquids, solids [80]. The fibers at the optimum stages were selected to measure their elemental content to validate the stages.

3.3.3.4. Thermal analysis. Thermal- gravimetric analysis (TGA) are imperative methods of determining the thermal stability of the functional groups in a sample. The TGA measures the amount of weight loss as a function of increasing temperature. A mass of 10-20 mg of ACFs were placed in a ceramic crucible for testing. The ACFs were heated from 30°C up to 900°C with a heating rate of 10°C/min at a nitrogen flow of 20 mL/min. The ACFs were held constant at 900°C for 10 minutes. The results obtained were used to develop both Thermo-Gravimetric (TG) and Differential Thermo-Gravimetric (DTG) curves for analysis. The TGA is used to analyze the contaminated Syn-ACFs with 350ppm of p-cresol. It was tested and placed in the crucible to run a desorption process of p-cresol.

3.3.4. Preparation of waste stream and calibration.

3.3.4.1. Standard phenol solutions. A p-cresol stock solution of 500 ppm was prepared by dissolving 0.5 g of p-cresol in 1000 mL of deionized water. Standard solutions (5 to 100 ppm) were prepared by diluting the stock solution samples to appropriate levels to provide suitable absorbance reading on UV-Vis spectrophotometer. The absorbance of these standard solutions on UV-Vis spectrophotometer at a wavelength of 278 nm was used to prepare the calibration curve.

3.3.4.2. Produced water. Stable emulsion, to mimic industrial produced water, was prepared using 1:25 v/v ratio of surfactant to deionized water. The surfactant and deionized water were added in required quantities and stirred for homogeneity. Produced water was prepared by adding identified amounts of heavy crude oil to the emulsion and stirred to homogeneity. Calibration curve for oil content was prepared by mixing known amounts of oil in n-hexane and read on UV-Vis spectrophotometer at a wavelength of 245 nm. In batch bench-scale experiments, the optimum parameters

obtained from the p-cresol adsorption were used to study the treatment of produced water by Syn-ACFs. The suspension was filtered using 0.45 μm syringe filters and a known volume of filtrate was stirred with n-Hexane (3 times) for oil extraction from the samples. The UV-Vis Spectroscopy at a wavelength of 245 nm was used to quantify the oil content [32].

3.3.5. Adsorption studies – isotherm and kinetics. Bench-scale batch studies were carried out for the removal of phenol and oil from aqueous streams using C-ACF, C-CF and Syn-ACFs to determine the optimum experimental conditions, kinetics and adsorption characteristics of the adsorbents (C-ACF, C-CF and Syn-ACFs).

The contact time, adsorbent dosage, pH and initial concentration of the synthesized wastewater were varied individually while keeping the other experimental conditions constant. In a typical experiment, known amount of adsorbent (0.1 – 2g/L) were added to 50 mL of phenol solution of different concentrations (50, 100, 200, 300, 400 and 500ppm) and stirred at 150 rpm for two hours at room temperature. Similarly, the contact time and pH were varied keeping the other experimental conditions constant. Analogous experimentation was carried out for produced water treatment using Syn-ACFs.

The removal efficiency of adsorbent from synthesized wastewater using Syn-ACFs was calculated from the following equation:

$$\text{Removal Efficiency} = \frac{C_0 - C_f}{C_o} * 100 \quad (14)$$

Where, C_o and C_f are the initial and final concentrations of the adsorbate before and after adsorption respectively.

Four adsorption isotherm models (Langmuir, Freundlich, Temkin and Dubinin-Radushkevich models) were correlated to the experimental data at optimum parameters to determine the adsorption characteristics and the applicability of the model. To investigate the adsorption kinetics, the experimental data were fitted to pseudo first order and pseudo second-order kinetic models. The amount of adsorbent adsorbed on the Syn-ACFs was calculated using the following equation:

$$Q_t = \frac{V(C_0 - C_t)}{M} \quad (15)$$

Where, Q_t is the amount of adsorbent adsorbed on the adsorbent at any time, C_o is the initial concentration of the adsorbate before adsorption while C_t is the concentration of adsorbate at any time during the adsorption. V and M represent the volume of the sample and mass of the adsorbent used, respectively.

3.3.6. Regeneration of Syn-ACFs. Chemical and thermal regeneration techniques were used to select the best method for effective Syn-ACFs regeneration. In the chemical regeneration, n- hexane and ethanol were evaluated to determine the effect of polarity to regenerate the Syn-ACFs. A weight of 1 g of Syn-ACFs were stirred with 20 mL of the solvent for 10 minutes. Afterwards, the Syn-ACFs were dried in the oven and reused further in the adsorption to determine the removal efficiency of p-cresol over different cycles. In thermal treatment, the ACFs were subjected to heat in the tube furnace after adsorption. The thermal regeneration was carried out at elevated temperatures of 400, 500 and 600^{o}C at a nitrogen flow rate of 135ml/min for 1 hour.

.

Chapter 4. Results and Discussion- Synthesis of ACFs

4.1. Stabilization

The fibers were yellow in color; during stabilization, the color changed from yellow to orange to red and finally black. At a temperature of 200ºC, the fiber color changed from yellow to orange in 7 hours stabilization without turning to black. The fibers shape and strength was confirmed; however, they weren't completely stabilized. Those orange fibers were tested using TGA in comparison with the black stabilized fibers. The TGA curves in appendix A.1 proved that at a temperature of 200ºC stabilization wasn't completed. The result showed that the orange fibers weren't thermally stable and showed a TG profile between the PAN fibers and the black stabilized fibers. On the other hand, evaluating the temperature at 300ºC as the stabilization temperature burned the fibers immediately as soon as they reach 300ºC. It was clearly observed without using SEM that the fiber structure was lost. The temperature at 250°C showed a promising results as a stabilization temperature, by which the fiber shape, strength, and color were confirmed. However, at a temperature of 250°C the fibers must be mixed while heating. This ensures the homogeneity of the fibers and avoid them to stick or burn. The TGA curves (see Appendix A.1) ensures the reproducibility of stabilization production line by which similar profiles revealed in each run.

4.2. Carbonization

The carbonization stage was tested without stabilization; however, the fibers were stuck together as one cluster and lost their strength. The result proved that stabilization is an essential stage. The experiment was carried out through the procedure mentioned in chapter 3 sections 3. Varying the temperature and fixing the flow rate to 135ml/min resulted in a change in the carbon content between the four experimented temperatures. The physical structure was studied using SEM (see Appendix A.4) the carbonized fibers using 850°C were in a good physical shape in comparison with 950°C carbonized fibers. Therefore, 850°C was selected as the optimum temperature for 2 hours with a nitrogen flow rate of 135ml/min. The TGA results (see Appendix A.1) verifies the reproducibility of the carbonization production line for three runs.

4.3. Activation

The carbonized fibers were activated using two methods as mentioned above, physical and chemical activation. The fibers were completely carbon, by activation the pores will form to enlarge the surface area. In CO_2 physical activation, the surface area of the samples obtained from various temperatures and flow rates were analyzed. As shown in table 5 the temperature at 950°C with a flow rate of 250ml/min proved high surface area around 774m^2/g at 2 hours. Nevertheless, the temperature of 850°C resulted in lower surface area around 173m^2/g. This could explain that activation temperature at 850°C wasn't sufficient to create the pores.

Table 5: Physical activation surface area using CO_2 at 850°C & 950°C at 2 hours.

Sample	Temperature °C	Surface area m^2/g
1	850	173
2	950	774

In chemical activation, KOH was selected upon other chemicals due to its promising results in many research papers [81, 82]. The results of the surface area using KOH ratio variation was determined using BET and summarized in the table below. As shown in table 6 that as the KOH mass ratio increases the surface area of the fibers increases. This explains the chemistry behind using KOH, by which it improves the itching in the activation process and creates porous structure [83, 82].

Table 6: Syn-ACFs KOH ratio and surface area at 950°C for 1 hour.

ACFs KOH ratio (wt:wt)	Surface area m^2/g
KOH 1:1	1356
KOH 2:1	2470
KOH 3:1	2889

Chapter 5. Characterization of C-ACFs and Syn- ACFs

5.1. Thermo-gravimetric Analysis

The thermo-gravimetric curves (TGA) presents the peak curves and their weight losses according to the breakdown of the surface groups at elevated temperatures. The TGA curves of PAN, stabilized 250ºC and carbonized 850ºC are shown in figure 2. The TG figure below, shows that PAN fibers aren't thermally stable compared to the carbonized fibers. This is explained by the temperature used in the production of the carbonized fibers, by which the functional groups were decomposed at 250°C in stabilization and between 250°C to 800°C in carbonization. The weight loss between 125-250°C could be explained due to the release of CO_2 gases along with nitrogen and air atmosphere during the dehydrogenation reactions [84, 85]. The other weight losses at multi stages is explained by PAN composition by which Hydrogen, HCN, and NH decomposed [85]. The DTG curves as shown in figure 3 proves the curves presented in the TG curves by which the carbonized fibers maintained thermal stability and ready for activation.

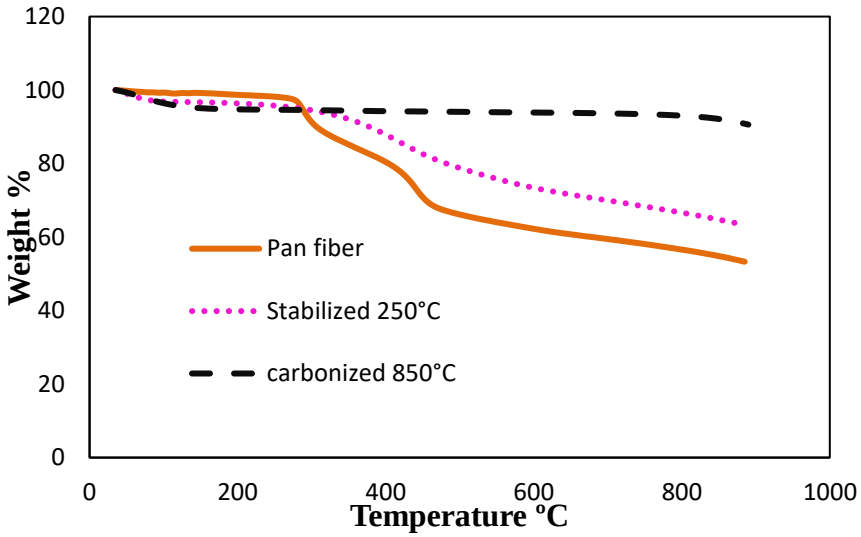

Figure 2: Thermo-gravimetric curves representing the percentage (%) weight loss for PAN, stabilized 250°C and carbonized 850°C.

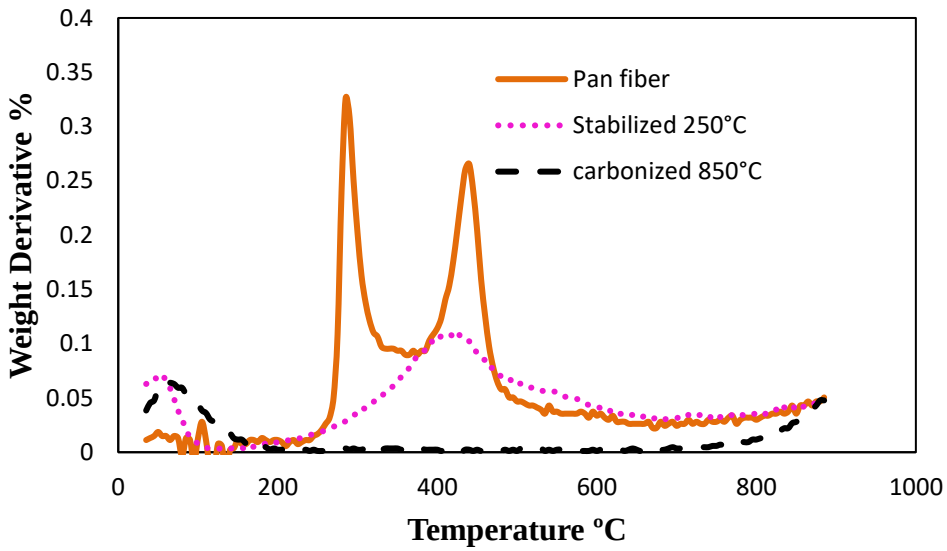

Figure 3: Differential thermo-gravimetric curves representing the derivative weight percentage (%) of PAN, stabilized 250°C and carbonized 850°C.

In figure 4, the Syn-ACF shows a higher weight loss at 100°C compared to other fibers. The DTG curves in figure 5 shows that the highest peak is found in the Syn-ACFs (KOH) compared to other fibers. This explains that syn-ACFs (KOH) has more pores carrying water content in contrast to other fibers. However, all fibers maintained thermal stability from 100-800°C, due to the production temperature.

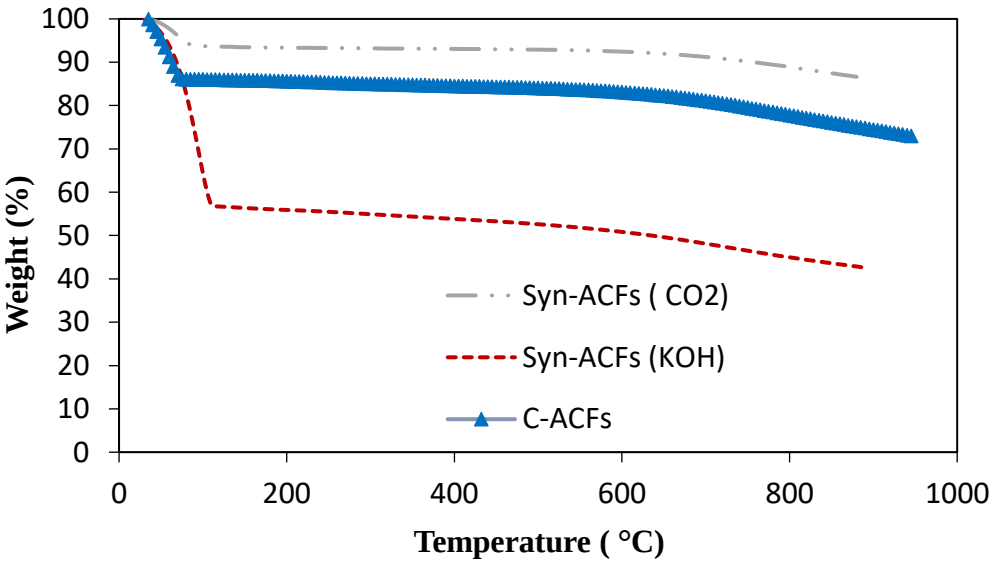

Figure 4: Thermo-gravimetric curves representing the percentage (%) weight loss for Syn-ACFs (CO_2), Syn-ACFs (KOH) and C-ACFs.

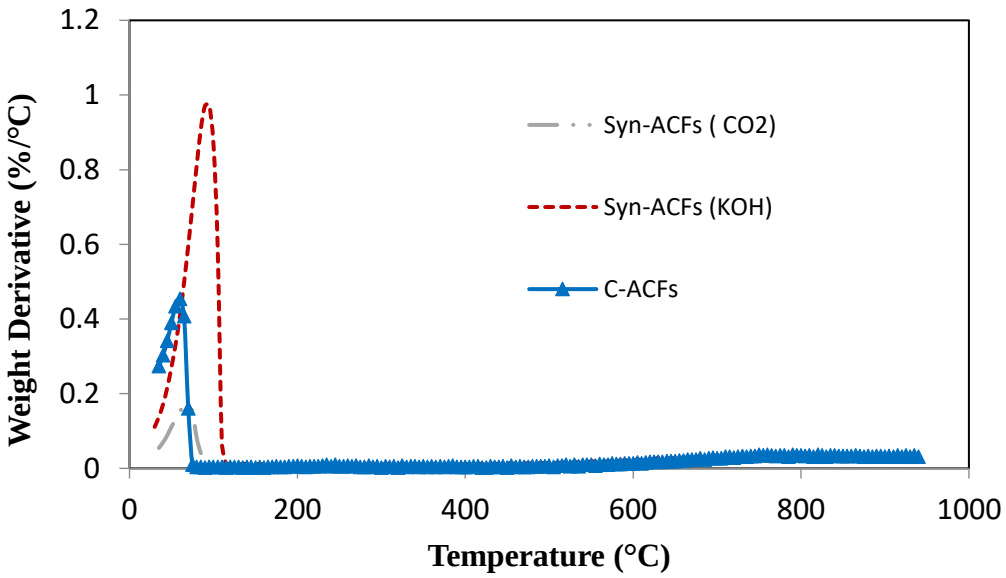

Figure 5: Differential thermo-gravimetric curves representing the derivative weight percentage (%) of Syn-ACFs (CO_2), Syn-ACFs (KOH) and C-ACFs.

5.2. CHN Analyzer

Table 7: CHN data elements of PAN, carbonized Syn-ACFs (KOH).

Sample Name	(N) %	(C) %	(H) %
PAN	23.31	66.16	5.638
Carbonized	0	71.77	1.511
Syn-ACFs (KOH)	0	86.05	1.353

The data in table 7 above, revealed the amount of nitrogen, carbon and hydrogen presented in each sample throughout the selected main stages of the ACFs synthesis. Table 7 shows that the carbon content increased from 66.16 % to 86.1 % as the fibers were activated and other elements decreased. These trends in the elemental analysis of carbon and other elements during carbonization are analogous to the results indicated in the literature [86].

5.3. Sorption of Nitrogen

Studying the surface structure is an essential parameter in the adsorption study of ACFs especially when the removal of trace concentration occurs to small molecules. The nitrogen adsorption isotherm using DFT allows the evaluation of the structural parameters besides the pore size distribution of the ACFs. Figure 6 explains the DFT isotherm of the volume increase with the relative pressure. The figure shows that the C-ACF is saturated at a relative pressure of 0.4 while the Syn-ACFs is saturated at a higher relative pressure 0.6. In addition, the figure shows the absence of hysteresis between the adsorption and desorption curve at the end in both samples which indicates that the volume is highly micropores. The graph reveals a higher volume increase in Syn-ACFs compared to C-ACFs, this result is due to the high surface area in Syn-ACFs.

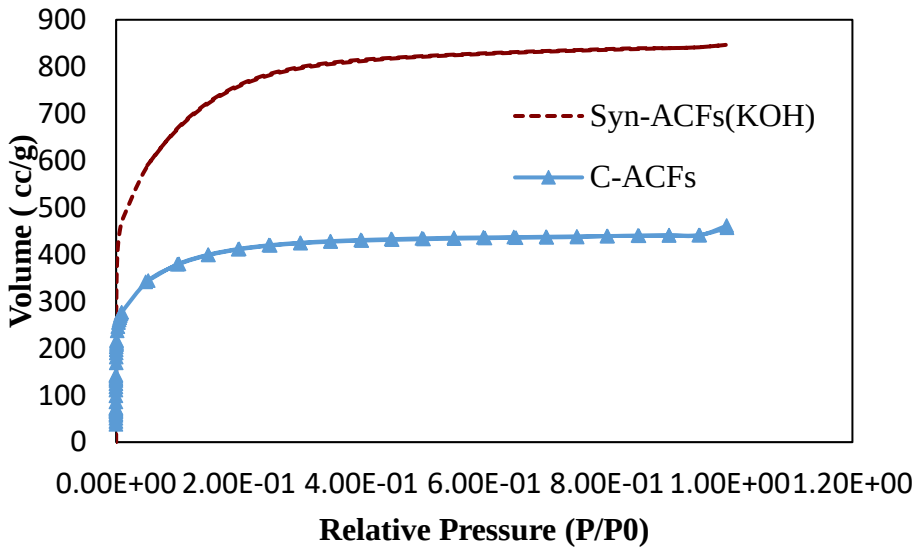

Figure 6: Nitrogen sorption isotherms at -196°C of Syn-ACFs (KOH) and C-ACFs.

The porosity is explained in details using figure 7 as a pore size distribution changes for both fibers. The figure supported the DFT isotherm in figure 6, due to the pore size range which is less than 20 Å. Since the range of the volume is between 10-20Å the volume is described to be micropores for both fibers. However, the dominant micropores volume as shown in figure 7 were given by Syn-ACFs (KOH). In micropores, high intermolecular force would be found due to the adjacent distance of pore walls to achieve high adsorption kinetic rate [42].

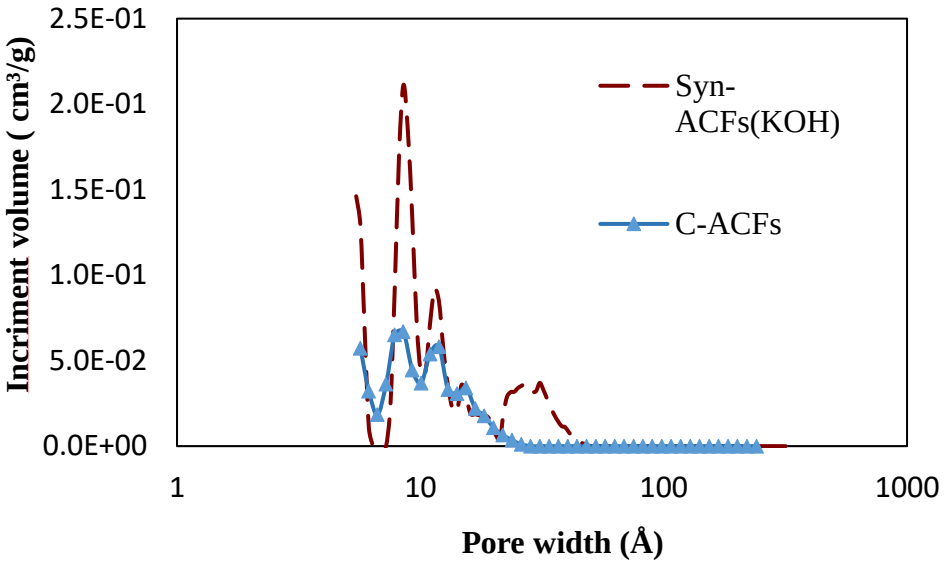

Figure 7: Pore size distributions of C-ACFs (KOH) and Syn-ACFs.

The DFT isotherm allows us to calculate the structural parameter such as ACF surface area S_{DFT}, the total volume of the pores V_t , the volume of the pores less than 20 Å $V_{<20Å}$ (micropore volume), and the volume of the pores less than 10 Å $V_{<10Å}$. Table 8 summarizes the structural parameters and supported the curves presented in the figures showing that most of the volume is in the micropores range for both fibers. In addition to highest total volume 2.39 and surface area given 2885 m^2/g were given by Syn-ACFs (KOH).

Table 8: Structural parameters of C-ACFs and Syn-ACFs calculated from nitrogen adsorption isotherms.

Sample	S_{BET} (m^2/g)	V_t (cm^3/g)	$V_{<20Å}$ (cm^3/g)	$V_{<10Å}$ (cm^3/g)
Syn-ACFs (KOH)	2885	2.39	1.87	1.24
C-ACFs	1500	0.633	0.612	0.318

5.4. SEM & EDS

The SEM was done to characterize the final structural surface of Syn-ACFs (KOH), Syn-ACFs (CO_2) and C-ACFs. Figure 8 shows the three fibers surface, by which it is shown that the synthesized fibers (a) and (b) maintained a good physical structure as the C-ACFs (c).

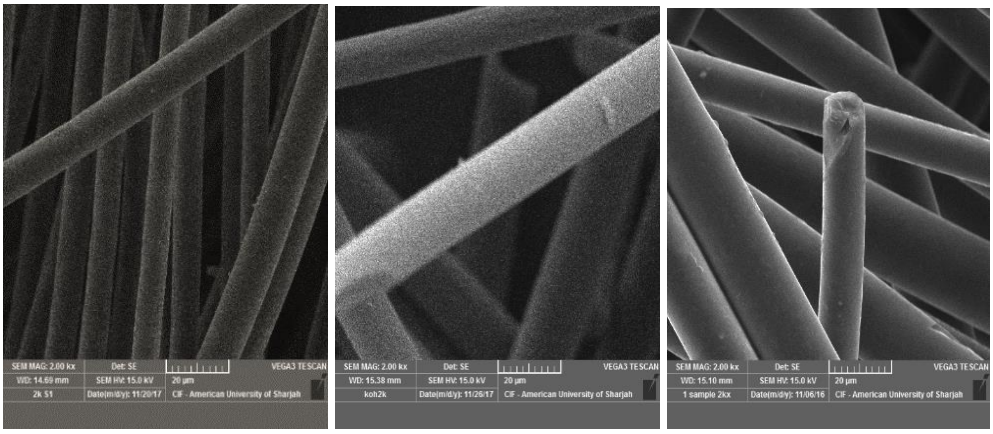

(a) (b) (c)

Figure 8: SEM images of Syn-ACFs (CO_2) (a), Syn-ACFs (KOH) (b) and C-ACFs (c).

The EDS allows us to figure out the composition of each sample. Table 9 shows the EDS analysis on Syn-ACFs(CO2), Syn-ACFs(KOH) and C-ACFs. According to spectrum selected the C-ACFs carbon content was higher 99% compared to the synthesized ACFs. The sulfur content appeared in a small ratio in C-ACFs this might be because of some residue during the production of the fibers. The Syn-ACF(KOH) s carbon content was around 88.5% which is less content in comparison with Syn-ACFs (CO_2).

Table 9: EDS analysis on Syn-ACFs (CO_2), Syn-ACFs (KOH) and C-ACFs.

Sample	O (%)	C(%)	S(%)
Syn-ACFs (CO_2)	9.9	91	-
Syn-ACFs (KOH)	11.5	88.5	-
C-ACFs	-	99	0.99

Chapter 6. Results and Discussion- Adsorption

6.1. Calibration curve

Figure 9 represents the absorbance spectra of p-cresol at varying concentration. It is evident from figure 9 that an increase in cresol concentration results in increased absorbance of the sample. Figure 10 represents the plot of absorbance values at different p-cresol concentrations. The p-cresol peak is evident at 278 nm even at low concentrations. Thus, the calibration curve was plotted at the peak value of 278 nm. The R^2 value of the linear curve generated, as shown in figure 10, was found to be 0.999 indicating the accuracy and precision of the calibration curve for quantification of p-cresol in aqueous solutions.

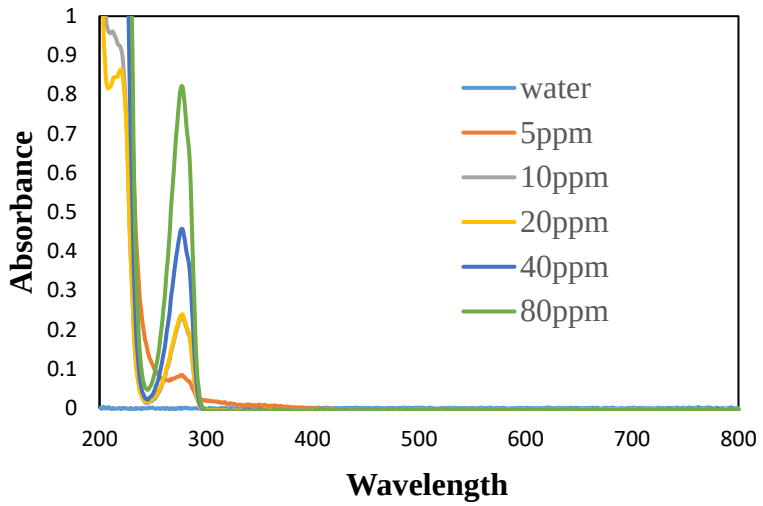

Figure 9: Spectra of cresol at varying concentrations.

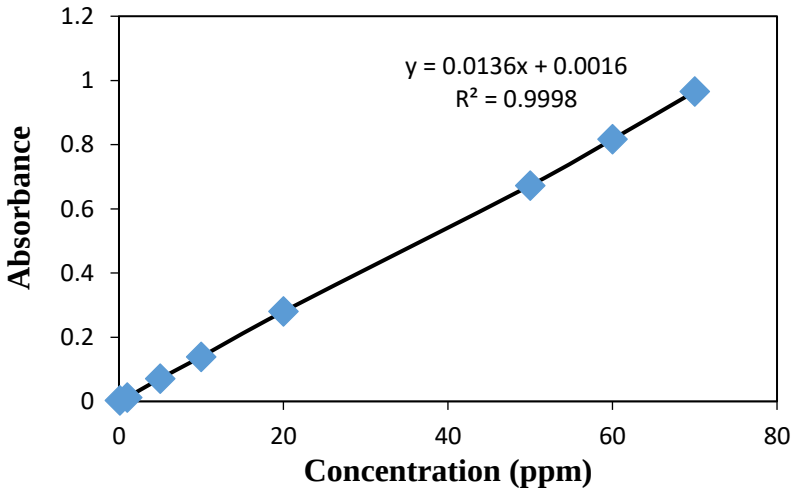

Figure 10: Cresol concentration calibration curve at $\lambda = 278$

6.1.1. C-ACF & C-CFs adsorption. Figure 11 represents a comparison of removal efficiency of cresol using C-ACF and C-CF at similar experimental conditions. As apparent from figure 11, C-CFs are unsuitable for p-cresol removal from aqueous solutions. On the other hand, C-ACF showed removal efficiencies of cresol exceeding 93% at a concentration of 150ppm. This points out towards the applicability of C-ACF in treating p-cresol contaminated wastewater streams. This high removal efficiency can be attributed to the high porosity and high surface area (1500m^2/g) of the C-ACF providing a large number of adsorption sites for p-cresol.

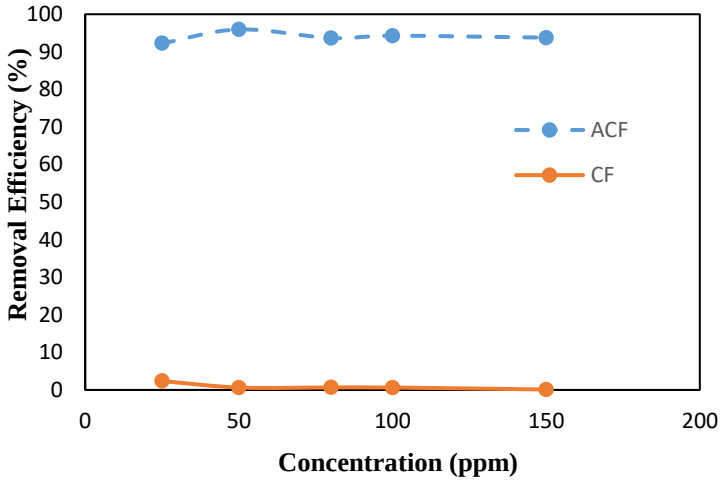

Figure 11: Comparison between the C-ACF and C-CF concentration effect of in the removal of p-cresol. Temperature = 25 °C, contact time = 30 min, absorbent dosage = 1.5 g/l, shaking rate = 150 rpm and initial pH = 4.6.

6.1.2. Effect of contact time. Figure 12 depicts the effect of time on the removal efficiency of p-cresol using C-ACFs and Syn-ACFs. The adsorption of cresol was carried out at the initial cresol concentration of 200 ppm (C-ACFs) and 350 ppm (Syn-ACFs). Other adsorption conditions were the adsorbent dosage of ACFs, shaking speed of 150 rpm and a temperature of 25°C. No increase in removal efficiency was observed after 30 minutes. Thus, the optimum contact time was selected to be 30 minutes to ensure that the system attains equilibrium and have maximum removal efficiency at given experimental conditions. Comparatively, the contact time for other conventional processes for phenol removal is several hours and even days, such as the biological treatment, compared to 30 minutes using ACFs.

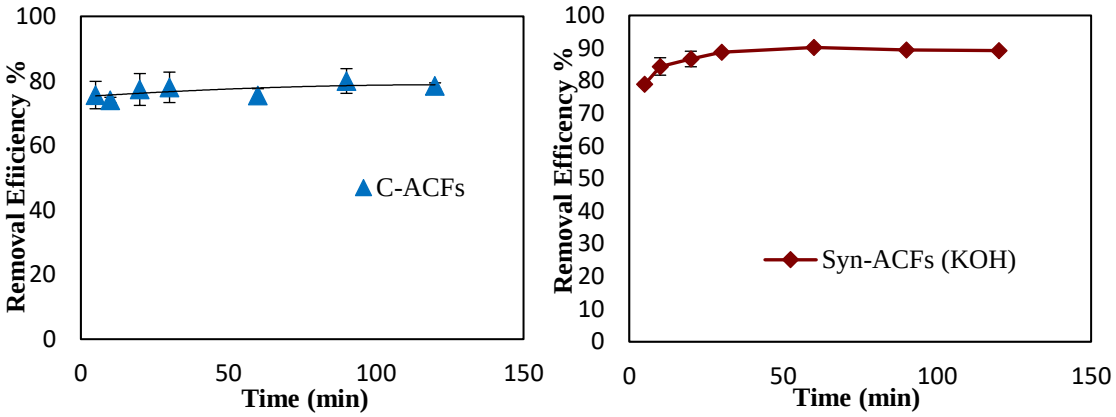

Figure 12: The effect of contact time on the removal efficiency of p-cresol by C-ACF and Syn-ACFs. Initial concentration = 200 ppm (C-ACF) and 350 ppm (Syn-ACF (KOH)), temperature = 25 °C, adsorbent dosage of ACFs = 1 g/l, shaking rate = 150 rpm and initial pH = 4.6.

6.1.3. Effect of adsorbent dosage. The effect of adsorbent dosage on the removal efficiency of p-cresol is shown in figure 13. The experimental conditions in terms of pH, time and temperature and were 4.6, 30 minutes and 25^{o}C, respectively. Figure 13 demonstrates an increase in removal efficiency of p-cresol as the adsorbent dosage is increased from 0.2 to 2 g/L. This sharp increase in the removal efficiency with increased adsorbent dosage is related to the increase in the available adsorption sites, initially. At adsorbent dosage less than 1.5 g/L, the effect of higher adsorption sites is decreased which can be explained in terms of equilibrium and the reduced availability of openly available sites [87, 88]. According to the results in figure 13, the optimum adsorbent dosage was selected to be 1.5 g/L and 1 g/L for C-ACFs and Syn-ACFs, respectively.

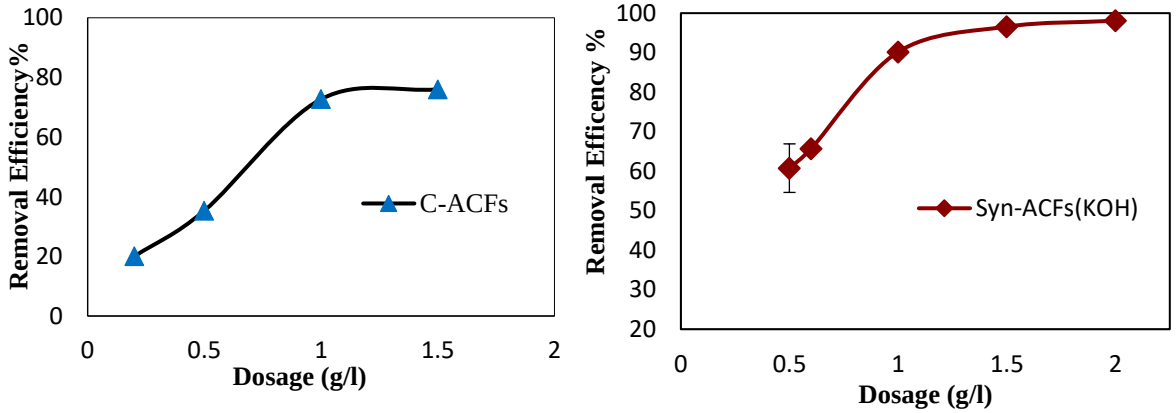

Figure 13: The effect of the amount of C-ACFs and Syn-ACFs (KOH) on the removal efficiency of p-cresol. Initial concentration = 200 ppm C-ACFs and 350 ppm Syn-

ACF s (KOH), temperature = 25 °C, contact time = 30 minutes, shaking rate = 150 rpm and initial pH = 4.6.

6.1.4. Effect of pH. The adsorption efficiency of phenols on the adsorbents is greatly affected by the pH of the solution which affects the phenol form in the solution and the adsorbent's surface charge [87]. The adsorption of phenol on Syn-ACFs was carried out at different pH ranging from 2 to 10 with constant parameters of adsorbent dosage, contact time, p-cresol initial concentration, shaking speed and temperature. Figure 14 demonstrates the initial pH influence on the adsorption of p-cresol on Syn-ACFs (KOH). This figure shows that the removal efficiency of p-cresol using Syn-ACFs (KOH) is highly pH dependent and decreased in the basic media. The decrease in the removal efficiency of phenol in alkaline media is due to the increased negative charge on the adsorbent surface [89]. The removal efficiency was higher in the region between the pH ranges of 4-7, this is due to the decrease in the static repulsion forces in the acidic region which enhanced the adsorption of p-cresol. The experimental results suggest the optimum pH to be within the pH ranges of 4-7.

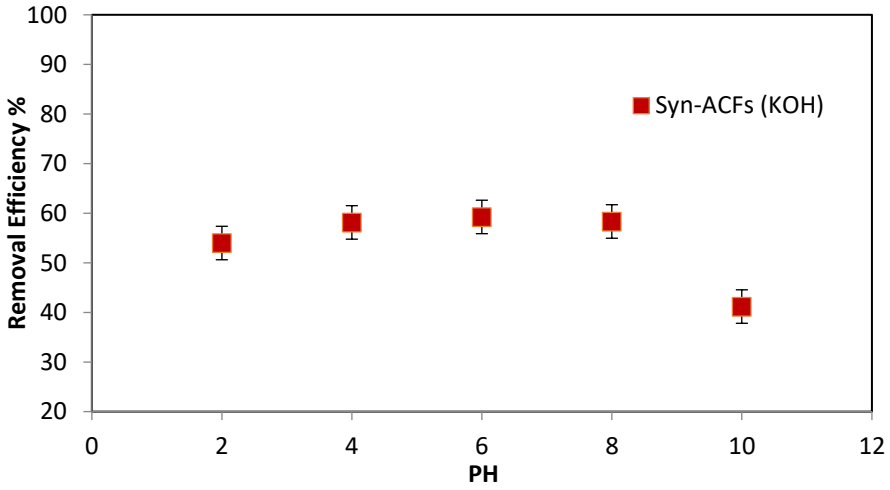

Figure 14: The effect of pH on the removal efficiency of p-cresol using Syn-ACFs (KOH). Initial concentration = 350 ppm, temperature = 25 °C, contact time =30 minutes, shaking rate = 150 rpm and adsorbent dosage = 0.5 g/l.

6.1.5. Effect of initial concentration of p-cresol. Figure 15 represents the removal efficiency of p-cresol from aqueous solution as a function of initial cresol concentration for both adsorbents C-ACF and Syn-ACFs (KOH). The decrease in the removal efficiency of p-cresol at increasing initial p-cresol concentration is due to the saturation of the adsorption sites in high p-cresol concentrations. Moreover, Syn- ACFs

(KOH) adsorption capacity is higher in comparison with the C-ACFs. This is due to the difference in surface area and pore size distribution compared to C-ACFs.

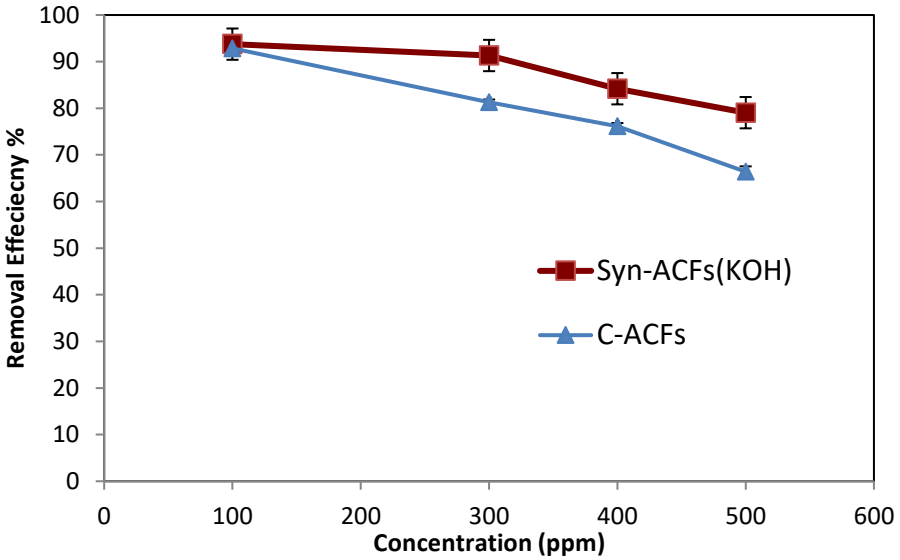

Figure 15: Concentration effect on the removal efficiency of cresol using the Syn-ACFs and C- ACFs. Temperature = 25 °C, contact time = 30 minutes, adsorbent dosage of 1 g/l, shaking rate = 150 rpm and pH = 4.6.

6.2. Adsorption isotherm models

The study of adsorption equilibrium and isotherms is vital to understand the adsorption characteristics. This corresponds to the adsorption capacity of the adsorbent, to the adsorbate concentration in the solution [87]. Several adsorption isotherms and models have been reported in literature [90, 91].

The equilibrium data are fitted using the four isotherms:

Langmuir isotherm (Equation 3).

Freundlich isotherm (Equation 5).

Temkin isotherm (Equation 6).

Dubinin- Radushkevich (D-R) isotherm (Equation 7).

Figures 16-19 depicts the comparison of adsorption isotherms of C-ACFs and Syn-ACFs for the four isotherms. Figure 16-19 shows good linear fit with regression coefficient (R^2) values ranging from 0.9972 to 0.9421 in all cases. However, Langmuir isotherms present the best fit of 0.9968 and 0.9972 for C-ACF and Syn-ACFs, respectively. This points towards the applicability of Langmuir isotherms for the adsorption of cresol on C-ACFs and Syn-ACFs with maximum adsorption capacity of

294 and 500 mg/g at room temperature, respectively. The increased adsorption capacity of Syn-ACFs can be attributed to the increased surface area during activation. Langmuir adsorption isotherm is developed to fit gas-solid adsorption to ACFs by which it is used to compare and measures the removal efficiency of different sorbents. Since it fits Langmuir the adsorption isotherm it is assumed that adsorption happens at fixed restricted number of sites with a molecular adsorption thick layer (monolayer adsorption). The R_L value of the C-ACFs, and Syn-ACFs (KOH) was calculated to be 0.026 and 0.044, which indicates that it's a favorable adsorption according to table 3 [92]. The detailed adsorption isotherm parameters are presented in Table 10.

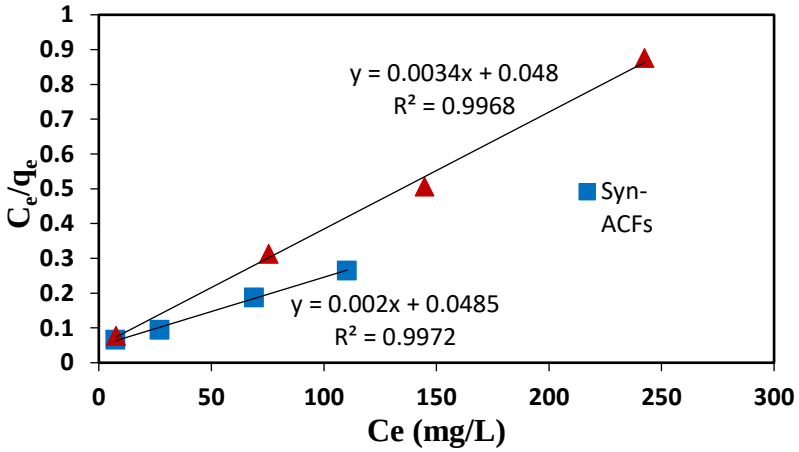

Figure 16: Langmuir adsorption isotherm for adsorption of cresol on Syn-ACFs and C-ACFs. Initial concentration = 350 ppm, temperature = 25.0 °C, adsorbent dosage = 1 g/L, contact time = 30 minutes, shaking rate = 150 rpm and initial pH=4.6.

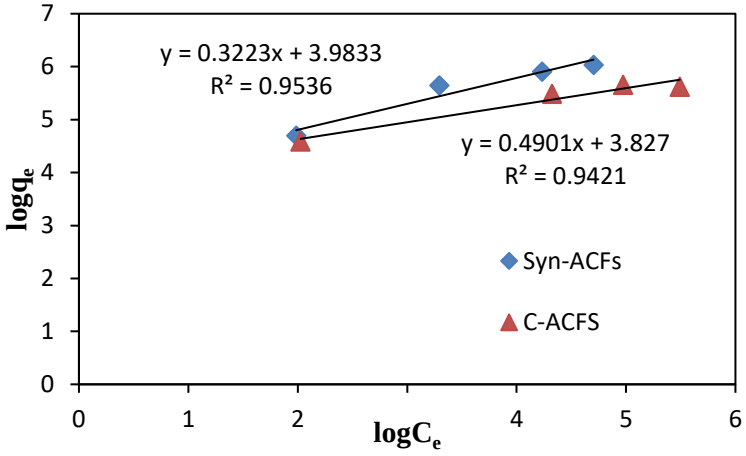

Figure 17: Freundlich adsorption isotherm for adsorption of cresol on C-ACFs and Syn-ACFs. Initial concentration = 350ppm, temperature = 25.0 °C, adsorbent dosage = 1 g/L, contact time = 30 minutes, shaking rate = 150 rpm and initial pH = 4.6.

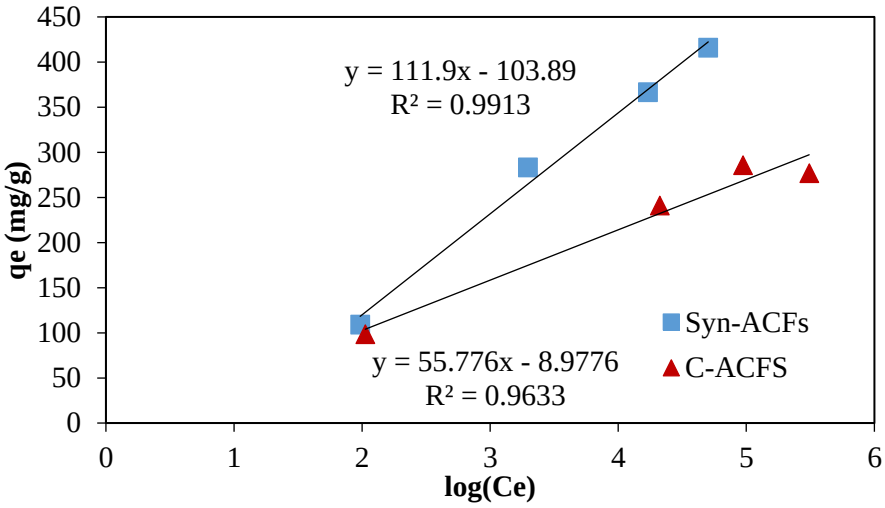

Figure 18: Temkin adsorption isotherm for adsorption of cresol on C-ACFs and Syn-ACFs. Initial concentration = 350 ppm, temperature = 25°C, adsorbent dosage = 1 g/L, contact time = 30 minutes, shaking rate = 150 rpm and initial pH = 4.6.

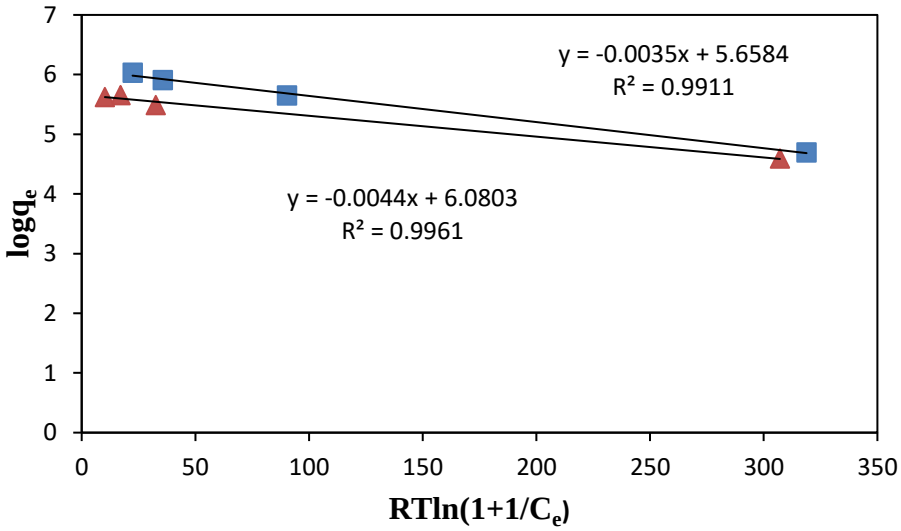

Figure19**:** Dubinin-Radushkevich adsorption isotherm for adsorption of cresol on ACFs. Initial concentration =350 ppm, temperature = 25°C, adsorbent dosage = 1g/L, contact time = 30 minutes, shaking rate = 150 rpm and initial pH = 4.6

Table10 : Values of isotherm constants for the removal of phenol using C-ACFs and Syn-ACFs (KOH).

Isotherm model	Parameters	C-ACFs values	Syn-ACFs (KOH) values
Langmuir	q_m $(\frac{mg}{g})$	294	500
	K_a $(\frac{l}{mg})$	0.0708	0.041
	R^2	0.9968	0.9972
Freundlich	K_F $(\frac{m^{(1-\frac{1}{n})}L^{\frac{1}{n}}}{g})$	53.69	45.92
	n_F	3.093	2.040
	R^2	0.9536	0.9421
Tempkin	B $(\frac{J}{mole})$	55.78	111.9
	K_t $(\frac{L}{mg})$	0.690	0.1198
	R^2	0.9633	0.9913
D-R	B_D	0.059	0.066
	R^2	0.9911	0.9961

6.3. Adsorption Kinetics

The study of the effect of contact time on the removal efficiency of cresol using C-ACFs and Syn-ACFs is of prime importance to determine the equilibrium time and adsorption rates. Figure 20 shows the relationship between adsorbed cresol to the contact time at room temperature and optimum conditions. The experimental data were fitted to two mainly used kinetic models – pseudo first order and pseudo second-order kinetic models. Figure 21 and 22 shows the linear forms of both kinetic models. The regression coefficients (R^2) values were 0.999 for pseudo second-order kinetic model in case of both adsorbents, respectively. This suggests that the adsorption of p-cresol on Syn-ACFs follows pseudo second-order reaction kinetics with rate constant of 0.540(g/mg.h). This indicates that that the reactions occurs at high ratio of sorbate/sorbent. The high ratio led to a chemical bonding that directs to an inclination towards a chemisorption reaction rather than a physisorption [93]. Table 11 provides the kinetic parameters for the two kinetic models discussed.

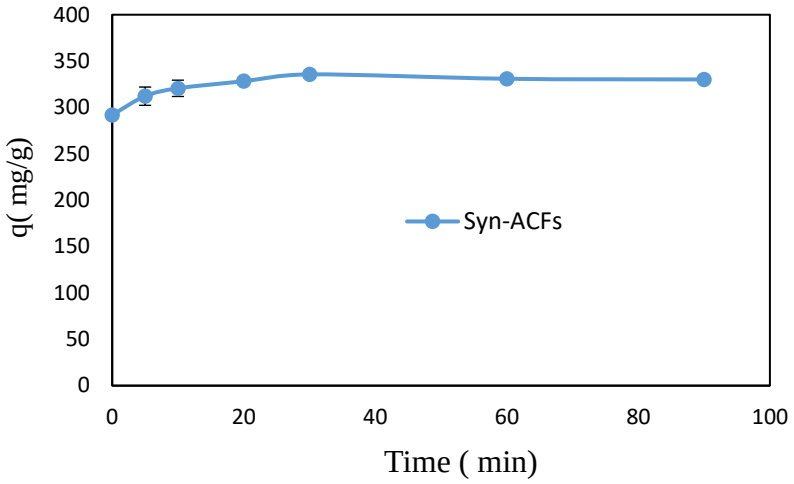

Figure 20: Amount adsorbed with respect to time for adsorption of cresol on Syn-ACFs. Temperature = 25°C, adsorbent dosage = 1g/l, shaking rate = 150 rpm, initial concentration = 350mg/l and initial pH = 4.6.

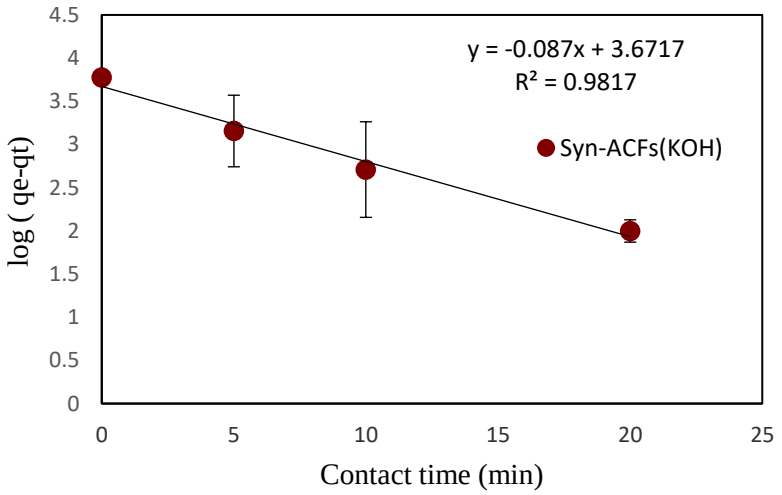

Figure 21: Pseudo-first-order kinetic model for adsorption of Syn-ACFs. Temperature = 25.0 °C, adsorbent dosage = 1 g/l, contact time = 30 minutes, initial concentration = 350 mg/l and shaking rate = 150.

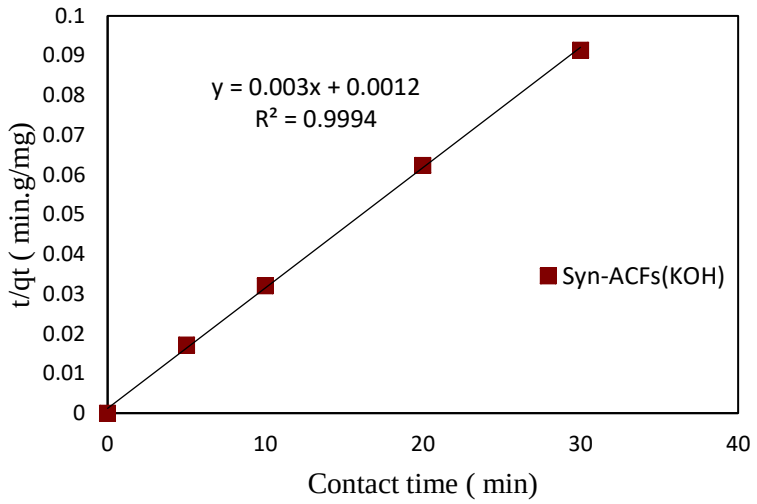

:

Figure 22: Pseudo- second-order kinetic model for adsorption on Syn-ACFs. Temperature = 25.0 °C, adsorbent dosage = 1 g/l contact time = 30 minutes and shaking rate = 150 rpm.

Table 11: Kinetic study on the adsorption of p-cresol Syn-ACFs (KOH) parameters.

ACFs	Kinetic Model	Parameter	Value
Syn-ACFs	Pseudo first order	K_I (g/mg.h)	5.22
		R^2	0.981
	Pseudo second order	K_{II} (g/mg.h)	0.540
		R^2	0.999

6.4. Syn- ACFs regeneration study

Figure 23-25 illustrates the comparison of regeneration impact on the removal efficiency of p-cresol using chemical and thermal regeneration techniques. In Figure 23 the regeneration using two solvents ethanol and n-hexane were evaluated to determine the effect of polarity on the regeneration of ACFs. It was shown above that n-Hexane provided higher removal efficiency compared to ethanol. This indicates that nonpolar solvent was effective since it provided a removal efficiency of 73%. Figure 24, shows a comparison of the thermal regeneration at different temperatures 400°C, 500°C and 600°C. At 600°C the removal efficiency 84% which was high compared to other temperatures. This could be explained due to the microporisity of ACFs, by which it required higher energy to desorb p-cresol. Figure 25 compared the best chemical and thermal regeneration from the previous figures for two regeneration cycles. In each subsequent cycle, the removal efficiency of Syn-ACFs decreased. This can be attributed

to the fact that the p-cresol molecules adsorbed within the microporous structure are less likely to be desorbed easily and adhere to the pores in each cycle. However, thermal regeneration at 600°C is enhanced by the increased molecular energy and kinetics of the cresol molecules (boiling point of cresol = 201.8ºC), thus allowing it to desorb easily. These results indicate thermal regeneration of Syn-ACFs to be preferable as compared to regeneration using n-hexane in the chemical regeneration technique.

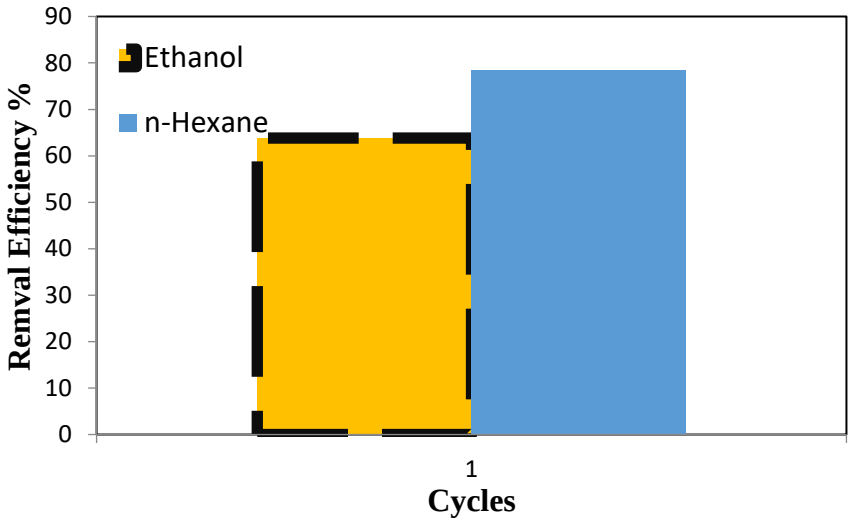

Figure 23: Regeneration study of Syn-ACFs on removal of p-cresol using solvent extraction n-Hexane and Ethanol. Initial concentration = 350 ppm, temperature = 25 °C, contact = 30 min, shaking rate=150 rpm and adsorbent dosage = 1 g/l.

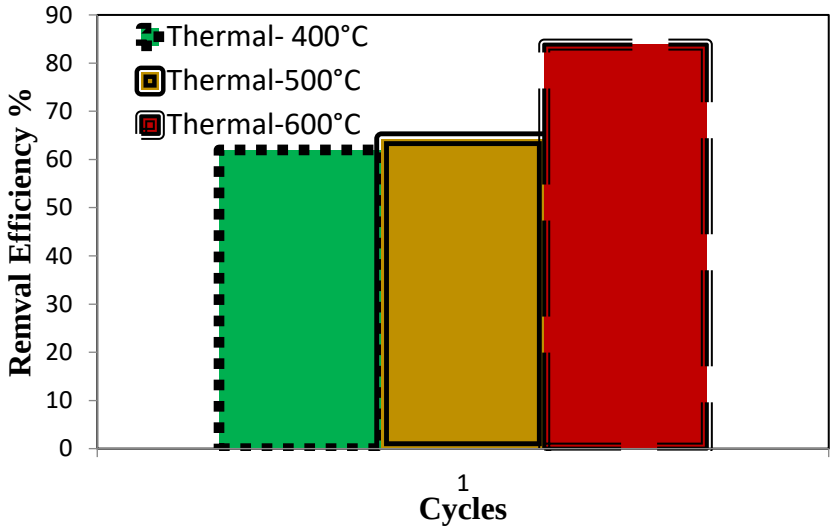

Figure 24: Regeneration study of Syn-ACFs on removal of p-cresol using thermal regeneration 400 ° C,500 °C and 600 ° C. Initial concentration = 350 ppm, temperature = 25 °C, contact = 30 min, shaking rate = 150 rpm and adsorbent dosage= 1 g/l.

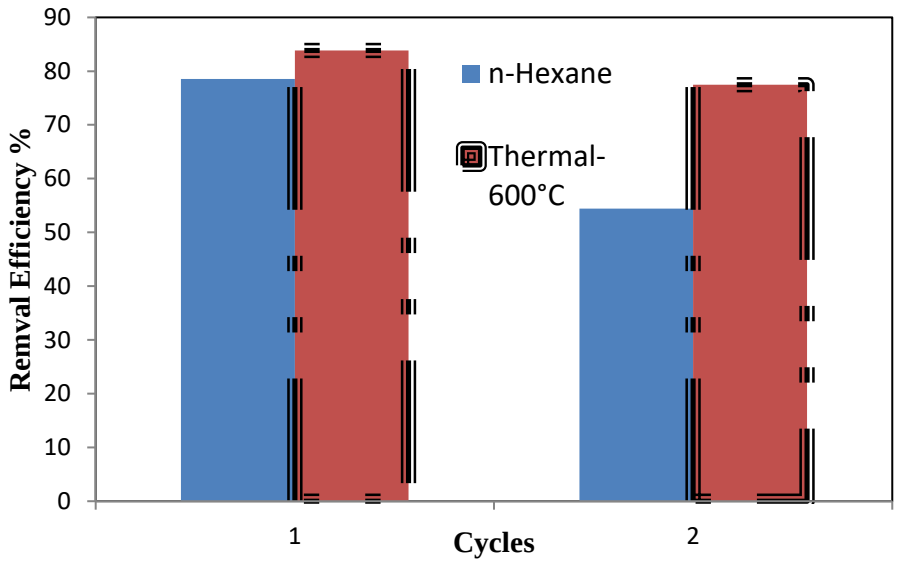

Figure 25: Regeneration study of Syn-ACFs on removal of p-cresol using chemical regeneration (n-Hexane) and thermal regeneration (600°C). Initial concentration = 350 ppm, temperature = 25 °C, contact time = 30 min, shaking rate = 150 rpm and adsorbent dosage = 1 g/l.

6.5. Adsorption of the synthesized produced water using Syn-ACFs

The Syn-ACFs were utilized for the treatment of synthesized produced water to determine their application in industrial produced water treatment systems. The synthesized produced water having an initial crude oil concentration of 200 ppm was mixed with Syn-ACFs at following experimental conditions (adsorbent dosage = 1 g/L, contact time = 2 hours, temperature = 25ºC, pH = 5.8, shaking rate = 150 rpm). The percent removal efficiency of oil using Syn-ACFs was determined to be 71.2 ± 1.3 %. This shows that the Syn-ACFs can be used effectively in industrial wastewater treatment applications.

Chapter 7. Conclusion and Recommendations

A complete literature review has been carried out throughout this thesis to highlight the significance of the adsorption technique and ACFs as an effective adsorbent in the removal of phenolic compounds. To conclude, a well-defined and optimized method was developed to synthesize ACFs. The stabilization process was proved to be an essential stage prior to carbonization. The stabilization temperature was selected to be 250°C with a time duration between 7-8 hours. The fibers must be mixed during stabilization to avoid burning and ensure homogeneity. In carbonization process the optimum parameters were found to be: Temperature = 850°C, time: 2 hours and a nitrogen gas flow rate of 135ml/min. The physical activation using CO_2 and the chemical activation using KOH were evaluated. The physical activation resulted in a surface area around 774m^2/g at a temperature of 950°C and a contact time of 2 hours. However, the chemical activation using a ratio of 3:1 KOH (wt/wt) gave a better surface area 2885m^2/g compared to 1:1 and 2:1 KOH (wt/wt) ratios. The developed ACFs surface area using KOH 3:1 (wt/wt) ratio achieved a high surface area 2885m^2/g compared to the C-ACFs1500 m^2/g. In a batch adsorption experiment the removal of p-cresol and emulsified oil from synthetic produced water was studied using Syn-ACFs (KOH). The results showed that Syn-ACFs (KOH) were capable to remove 91% of p-cresol with an initial concentration of 350ppm and were able to treat 71.2% of produced water contaminants at a concentration of 200ppm. The optimum parameters of Syn-ACFs in the removal of p-cresol were the following: Temperature = 25°C, time: 30min, adsorbent dosage: 1 g/l, shaking rate = 150 rpm and initial pH = 4.9. The Syn-ACFs (KOH) best isotherm model was found to fit Langmuir isotherm with an adsorption capacity of 500mg/g, whereas the adsorption kinetics were described by pseudo-second order with a rate of 0.540 (g/mg.min). The thermal regeneration at 600°C of the contaminated Syn-ACFs (KOH) with p-cresol achieved a higher removal efficiency of 84% compared to the chemical regeneration using n-hexane (78%).

For further experimentations, the ACFs synthesis might be completed using another type of precursor. A study of pilot scale is required to determine the feasibility of the synthesis method at a commercial scale.

References

[1] U. Nations, 2016. [Online]. Available: www.Sustainabledevelopment.un.org.

[2] "Increasing Demand and Climate Change Threaten Global Water Supplies UN Report," 12 March 2012. [Online]. Available: www.un.org/apps/news/story.asp?NewsID=41513&Cr=Water&Cr1=Sanitation#.WYo1adPyuCQ.

[3] A. Fakhru'l-Razi, A. Pendashteh, L. C. Abdullah, D. R. Biak, S. S. Madaeni and Z. Z. Abidin, "Review of Technologies for Oil and Gas Produced Water Treatment," vol. 170, pp. 530-551, 2009.

[4] L. BV, "Water Treatment Solutions," 2017. [Online]. Available: www.lenntech.com/aquatic/organic-pollution.htm. [Accessed 6 September 2017].

[5] S. K. Garg and D. R. Modi, "Decolorization of Pulp-paper Mill Effluents by White-Rot Fungi," *Critical Reviews in Biotechnology,* vol. 19, no. 2, pp. 85-112, 2008.

[6] H. SHI, "Industrial Wastewater-Types, Amounts and Effects," *Point Source of Pollution: Local Effects and It's Control,* vol. 1, 2009.

[7] "Enviromental Protection Agency (1984) Methods 604, Phenols in Federal Register," [Online]. Available: https://www.epa.gov/sites/production/files/2015-08/documents/method_604_1984.pdf. [Accessed 30 October 2016].

[8] H. Pasdar and R. Marandi, "Effect of Phenol Loading on Wastewater Treatment by Activated Sludge Process," *Journal of Basic and Applied Scientific Research,* vol. 3, no. 11, pp. 121-126, 2013.

[9] A. Vanjara and D. N. Jadhav, "Removal of Phenol From Wastewater Using Sawdustpolymerized Sawdust and Sawdust Carbon," *IndianJ. Chem. Technol,* vol. 11, pp. 35-41, 2004.

[10] S. J. Kulkarni and J. P. Kaware, "Review on Research for Removal of Phenol From Wastewater," *International Journal of Scientific and Research Publications,* vol. 3, no. 4, pp. 2250-3153, 2013.

[11] C. Anindita, B. Mekala, A. Sharma and N. Verma, "Preparation of Carbon Micro-/Nano Fibers for Adsorption of Dissolved Organic and Inorganic Solutes," in *Seperation Processes,* Allied Publishers Pvt.Ltd, 2009, pp. 13-20.

[12] “New Technologies in Phenol Removal From Wastewater,” 2016. [Online]. Available: http://www.oilgae.com/algae/cult/sew/new/phe/phe.html.

[13] K. Sharma, S. Kaur and M. Rana, “Studies on Differenet Methods for Removal of Phenol in Wastewater-Review,” *International Journal of Science, Engineering and Technology Research (IJSETR),* vol. 1, no. 6, 2016.

[14] E. Munaf, R. Zein, R. Kurniadi and I. Kurniadi, "The Use of Rice Husk for Removal of Phenol from Wastewater as Studied using 4-Aminoantipyrine Spectrophotometric Method," *Enviromental Technology,* vol. 18, pp. 355-358, 2010.

[15] C. Bertoncini, J. Raffelli, L. Fassino, H. Odetti and E. Botani, "Phenol Adsorption on Porous and Non-Porous Carbons," *Carbon,* vol. 41, no. 6, pp. 1101-1111, 2003.

[16] M. Khalid, G. Joly, A. Renaud and P. Mangnoux, "Removal of Phenol from Water by Adsorption using Zeolites," *Ind. Eng. Chem. Res.,* vol. 43, no. 17, pp. 5275-5280, 2004.

[17] S. V. Shobha and B. Ravindranath, “Supercritical Carbon Dioxide and Solvent Extraction of The Phenolic Lipids of Cashew nut (Anacardium Occidentale) Shells,” *J.Agric.Food Chem,* vol. 39, no. 12, pp. 2214-2217, 1991.

[18] N. Pradeep, S. Anupama, K. Navya, H. Shalini, M. Idris and U. Hampannavar, “Biological Removal of Phenol from Wastewaters: A Mini Review,” *Appl Water Sci,* vol. 5, no. 2, pp. 105-112, 2014.

[19] A. Hussaim, S. K. Dubey and V. Kumar, "Kinetic Study for Aerobic Treatment of Phenolic Wastewater," *Water Resources and Industry,* vol. 11, pp. 81-90, 2015.

[20] B. Marrot, A. Barrios-Martinez, P. Moulin and N. Roche, "Biodegradation of High Phenol Conentration by Activated Sludge in an Immersed Membrane Bioreactor," *Biochemical Engineering Journal,* vol. 30, no. 2, pp. 174-183, 2006.

[21] M. Stanisavljević and L. Neldic, "Removal of Phenol from Industrial Wastewaters By Horseradish (Cochlearia Armoracia L) Peroxidase," *Working and Living Environmental Protection,* vol. 2, no. 4, pp. 345-349, 2004.

[22] M. Masuda, A. Sakurai and M. Sakakibara, "Effect of Reaction Conditions on Phenol Removal by Polymerization and Precipitation using Coprinus Cinereus Peroxidase," *Enzyme and Microbial Technology,* vol. 28, no. 4-5, pp. 295-300, 2001.

[23] M. A. Zazouli and M. Taghavi, "Phenol Removal from Aqueous Solutions by Electrocoagulation Technology using Iron Electrodes: Effect of Some Variables," *Journal of Water Resource and Protection,* vol. 4, pp. 980-983, 2012.

[24] E.-S. Z. EL-Ashtoukhy, Y. A. El-Taweel, O. Abdelwahab and E. M. Nassef , "Treatment of Petrochemical Wastewater Containing Phenolic Compounds by Electrocoagulation Using a Fixed Bed Electrochemical Reactor," *Int. J. Electrochem. Sci.,* vol. 8, pp. 1534-1550, 2013.

[25] Z. Longfei, Y. Yong, W. Yuehui, Y. Liushui and L. Zhenfan, "Study on The Photodegradation of Phenol Containing Wastewater by La_(0.9)Ce_(0.1)MnO_3," *Enviromental Pollution and Control,* vol. 33, no. 6, pp. 7-10, 2011.

[26] G. Xiaoming, F. Feng1, L. Lei1, W. Yufei1, W. Jing1 and L. Wenhong2, "Reparation of Cu-BiVO4 Photocatalyst and its Application in The Treatment of Phenol-Containing Wastewater," *Chemical Industry and Engineering Progress,* vol. 31, no. 5, pp. 1039-1043, 2012.

[27] B. Marrot, A. Barrios-Martinez, P. Moulin and N. Roche, "Biodegradation of High Phenol Concentration by Activated Sludge in an Immersed Membrane Bioreactor," *Biochemical Engineering Journal,* vol. 30, pp. 174-183, 2006.

[28] J. V. Bevilaqua, M. C. Cammarota, D. M. G.Freire and G. L. Sant'AnnaJr, "Phenol Removal Through Combined Biological and Enzymatic Treatments," *Braz. J. Chem. Eng,* vol. 19, no. 2, 2002.

[29] L. Jiang and X. Mao, "Degradation of Phenol-containing Wastewater using an Improved Electro-Fenton Process," *nt. J. Electrochem. Sci.,* vol. 7, pp. 4078-4088, 2012.

[30] S. K. Dhidan, "Removal of Phenolic Compunds From Aqueous Solutions by Adsoption onto Activated Carbons Prepared From Date Stones by Chemical Activation with FeCl3," *Journal of Engineering,* vol. 18, no. 1, 2012.

[31] A. A. Ahmad and H. B. Hameed, "Reduction of COD and color of dyeing effluent from a cotton textile mill by adsorption onto bamboo-based activated carbon," *Journal of Hazardous Materials,* vol. 172, no. 2-3, pp. 1538-1543, 2009.

[32] L. Abou Chacra, "Treatment of Produced Water Using Graphene," M.S. thesis, Department of Chemical Engineering, American University of Sharjah, Sharjah, UAE, 2016.

[33] J. A. Balanay, "Adsorption Characteristics of Activated Carbon Fibers (ACFs) For Toluee," PhD. thesis, University of Alabama,Birmingham, 2011.

[34] B. H. Hameed, D. K. Mahmoud and A. L. Ahmad, "Equilibrium modeling and kinetic studies on the adsorption of basic dye by a low-cost adsorbent: Coconut (Cocos nucifera) bunch waste," *Journal of Hazardous Materials,* vol. 158, pp. 65-72, 2008.

[35] F. L. George and D. S. H., *Wastewater Engineering-Treatment and Reuse,* 4th Edition ed., 2003.

[36] B. Saha and C. Orvig, “Biosorbents for Hexavalent Chromium Elimination from Industrial and Municipal Effluents,” *Journal of Coordination Chemistry Reviews,* vol. 254, no. 23-24, pp. 2959-2972, Dec 2010.

[37] S. Gulistan, “"Oil Removal From Produced Water Using Natural Materials," M.S. thesis, Department of Chemical Engineering, American University of Sharjah,” Sharjah, UAE, 2014.

[38] J. Economy, “Flame-Retardant Polymeric Material,” *Carbon,* vol. 2, no. Plenum Publishing Corporation, pp. 203-226, 1978.

[39] T. Lee, C. H. Ooi, R. Othman and F. Y. Yeoh, "Activated Carbon Fiber - The Hybrid of Carbon Fiber and Activated Carbon," *Rev.ad.Mater.Sci.,* vol. 36, pp. 118-138, 2014.

[40] T. J. Mays, "Chapter 3- Activated Carbon Fibers," *Carbon Materials for Advanced Technologies ,* pp. 95-118, 1999.

[41] S. Kisamori, K. Kuroda, S. Kawano, I. Mochida, Y. Matsumura and M. Yoshikawa, "Oxidative Removal of SO2 and Recovery of H2SO4 over Poly(acrylonitrile)-Based Active Carbon Fiber," *Energy and Fuels,* vol. 8, no. 6, pp. 1337-1339, 1994.

[42] J. A. Balanay, A. A. Bartolucci and C. T. Lungu, "Adsorption Characteristics of Activated Carbon Fibers (ACFs) for Toluene: Application in Respiratory Protection," *Journal of Occupational and Environmental Hygiene,* vol. 11, no. 3, pp. 234-269, 2014.

[43] I. Mochida, Y. Korai, M. Shirahama, S. Kawano, T. Hada, Y. Seo, M. Yoshukawa and A. Yasutake, "Removal of SOx and NOx Over Activated Carbon Fibers," *Carbon,* vol. 38, no. 2, pp. 227-239, 2000.

[44] I. Mochida, S. Kawanao, S. Kisamori, H. Fujitsu and T. Maeda, "PAN based activate carbon fibers : Production,characterization and application," *Carbon,* vol. 32, pp. 175-189, 1994.

[45] P. Nousiainen, M. Nieminen, S. Heidari, A. Vuori, J. Laine and M. Juntuen, "Activated Carbon Fibers in Air and Water Purification,," Word Textile Congress, UK, 1994.

[46] H. T. Ko, P. Chiranairdul and H. C. Lin, "Carbon," *J Material Sci lett,* vol. 30, no. 4, pp. 647-655, 1992.

[47] P. Bajaj and A. Dhawan, “PAN-Based Activated Carbon Fiber: Production, Charectriztion and Application,” *Indian Journal of Fiber & Texile Research,* vol. 22, pp. 222-235, December 1997.

[48] E. G. Milioni, S. C. Anagnou, L. A. Kartsonakis and C. A. Charitidis, " Synthesis of New Carbon Fiber Precursors Using AGET ATRP in Microemulsion," 2015. [Online]. Available: https://pdfs.semanticscholar.org/5844/7eea6a382829bda3aeae3235b2b7ff986c7a.pdf.

[49] S.-J. Park and G.-Y. Heo, "Precursors and Manufacturing of Carbon," *Carbon Fibers,* vol. 210, pp. 31-66, 2015.

[50] C. Berrueco, P. Alvarez, N. Díaz, M. Granda, R. Menéndez,, C. Blanco, R. Santamaria and M. Millan, "High performance activated carbon for benzene/toluene adsorption from industrial wastewater," *Journal of Hazardous Materials,* vol. 192, no. 3, pp. 1525-1532, 2011.

[51] A. OYA and S. Yoshida, "Antibacterial Activated Carbon Fiber Ferived from Phenolic Resin Containing Silver Nitrate," *Carbon,* vol. 31, no. 1, pp. 71-73, 1993.

[52] S. Shiraishi, in *Carbon Alloys: Novel Concepts to Develop Carbon Science and Technolog*, Tokyo, Elsevier, 2003, pp. 447-479.

[53] K. Chung and T. Park, "Consistency condition of isotropic–kinematic hardening of anisotropic yield functions with full isotropic hardening under monotonously proportional loading," *International Journal of Plasticity,* vol. 45, pp. 61-84, 2013

[54] V. Jimenez, P. Sanchez and A. Romero, "Material for Activated Carbon Fiber Synthesis," in *Activated Carbon Fibers and Textiles*, Spain, Woodhead puplishing, 2016.

[55] J. Park and Y. G. Heo, "Precursors and Manufacturing of Cabron Fibers," *In: Springer Series in Material Science,* vol. 210, pp. 31-66, 2015.

[56] D.-n. Li and X.-j. Ma, "Preparation and Characterization of Activated Carbon Fibers from Liquefied Wood," *Cellulose,* vol. 20, no. 4, pp. 1649-1656, 2013.

[57] Y. Uraki, A. Nakatani, S. Kubo and Y. Sano, "Preparation of activated carbon fibers with large specific surface area from softwood acetic acid lignin," *J. Wood. Sci,* vol. 47, p. 465–469, 2001.

[58] I. A. Tan, A. L. Ahmed and B. H. Hameed, "Preparation of Activated Carbon from Coconut Husk: Optimization Study on Removal of 2,4,6- Trichlorophenol Using Response Surface Methodoly," *Journal of Hazardous Materials,* vol. 153, no. 1-2, pp. 709-717, 2008.

[59] A. R. Hidayu, N. F. Mohamad, S. Matali and A. Sharifah, "Characterization of Activated Carbon Prepared from Oil Palm Empty Fruit Bunch Using BET and FT-IR Techniques," *Procedia Engineering,* vol. 68, pp. 379-384, 2013.

[60] Y. Zaho, F. Fang, H.-M. Xiao, Q.-P. Feng, L.-Y. Xiong and S.-Y. Fu, "Preparation of Pore-Size Controllable Activated Carbon Fibers from Bamboo Fibers with Superior Performance for Xenon Storage," *Chemical Engineering Journal,* vol. 270, pp. 528-534, 2015.

[61] X. Ma, H. Yang, L. Yu, Y. Chen and Y. Li, "Preparation, Surface and Pore Structure of High Surface Area Activated Carbon Fibers from Bamboo by Steam Activation," *Materials,* vol. 7, no. 6, pp. 4431-4441, 2014.

[62] W. E. Marshall, L. H. Wartelle and D. E. Akin, "Flax Shive As a Source Of Activated Carbon For Mtals Remediation," *Bioresources,* vol. 2, no. 1, pp. 82-90, 2007.

[63] G.-X. Zhao, B.-J. Chen and S.-A. Qian, "Kinetics of the -C-N Bond Transformation into Conjugate -C-N Bond in Acrylonitrile Copolymer Using in SituFourier Transform Infrared Spectroscopy," *J. Anal. Appl. Pyrolysis,* vol. 23, no. 1 pp. 23-87, 1992.

[64] K. Minura, H. Nakagawa and K. Hashimoto, *Fibers and Composites*, vol. 33, London and NewYork: Taylor&Francis Group, 1995, pp. 247-348.

[65] M. C. Paiva, P. Kotasthane, D. D. Edie and A. A. Ogale, "UV Stabilization Route for Melt-Processible PAN-based Carbon Fibers," *Carbon,* vol. 41, no. 7, pp. 1339-1409, 2003.

[66] M. S. Rahaman, A. F. Ismail and A. Mustafa, "A Review of Heat Treatment on Polyacrylonitrile Fiber," *Polymer Degradation and Stability,* vol. 92, no. 8, pp. 1421-1432, 2007.

[67] A. Gupta and I. R. Harrison, "New Aspects in The Oxidative Stabilization of PAN-based Carbon Fibers," *Carbon,* vol. 34, no. 11, pp. 1427-1445, 1996.

[68] J. Mittal, R. B. Mathur, O. P. Bahl and M. Inagaki, "Post Spinning Treatment of PAN Fibers Using Succinic Acid to Produce High Performance Carbon fiber," *Carbon,* vol. 36, no. 7-8, pp. 893-897, 1998.

[69] T.-H. Ko, T.-c. Day and M.-F. Lin, "The Effect of Precarbonization on Mechanical Properties of Final Polyacrylonitrile-based Carbon Fibres," *Journal of Materials Science Letters,* vol. 12, no. 5, pp. 343-345, 1993.

[70] E. Fitzer and J. D. Muller, "The Influence of Oxygen on The Chemical Recations During Stabilization of pn as Carbon Fiber Precursor," *Carbon,* vol. 13, pp. 63-89, 1975.

[71] J. c. Lee, B. H. Lee, B. G. Kim, M. J. Park, D. Y. Lee, I. H. Kuk, H. Chung, H. Chung, H. S. Kang, H. S. Lee and D. H. Ahn, "The Effect of Carbonization Temperature of PAN Fiber on The Properties of Activated Carbon Fiber Composites," *Carbon*, vol. 35, no. 10-11, pp. 1479-1484, 1997.

[72] X. Bin, W. Feng, C. Gao-ping and Y. Yu-sheng, "Effect of Carbonization on Temperature on Microstructure of PAN-based Activated Carbon Fibers Prepared by Co2 Activation," *New Carbon Materials*, vol. 21, no. 1, pp. 21-25, 2006.

[73] M. El-Naas, S. Al-Zuhair and M. Alhaija, "Removal of Phenol from Petroleum Refinery Wastewater Through Adsorption on Date-pit Activated Carbon," *Chemical Engineering Journal*, vol. 162, no. 3, pp. 997-1005, 2010.

[74] L. C. Mangun, M. Daley and L. Economy, *88th Annual Meeting of Air & Waste Managment Association*, San Antonio: TX, 1995.

[75] S. Kulkarni and J. Kaware, "Removal of Phenol from Wastewater," *Interntional Journal of Scientific and Research Publications*, vol. 3(4), pp. 1-5, 2013.

[76] N. Briceño and M. Guzmán, "Grupos Superficiales en Materiales Carbonosos. Caracterización Por Diferentes Técnicas.," *Revista Colombiana de Química*, vol. 36, no. 1, pp. 121-130, 2007.

[77] A. Carvajal-Bernal, F. Gomez, L. Giraldo and P. Moreno, "Chemical Modification of Activated Carbons and its Effet on Adsportion of Phenolic Compounds," *Ingenieria Y Competitividad*, vol. 17, no. 1, pp. 109-119, 2015.

[78] A. Carvajal-Bernal, F. Gomez, L. Giraldo and J. Moreno-Piraja, "Chemical Modification of Activated Carbons and its Effect on the Adsorption of Phenolic Compounds," *Ingeneria Y Competitividad*, vol. 17, no. 1, pp. 109-119, 2015.

[79] Y. Elsayed, M. Khamis, F. Samara, M. Alqaydi, Z. Sara, I. Al Zubaidi and M. Mortula, "Novel Method for Water Purification Using Activated Adsrobents Developed from Sewage Sludge," *Desalination and Water Treatment*, vol. 57, no. 33, pp. 1-11, 2016.

[80] M. Thompson, "Royal Society of Chemistry," 2008. [Online]. Available: http://www.rsc.org/images/CHNS-elemental-analysers-technical-brief-29_tcm18-214833.pdf. [Accessed 21 11 2017].

[81] Y. Z. Xia, S. S. Huang, J. P. Cao, S. C. Xi, X. Y. Wei, J. Kamamtoto and T. Takarada, "KOH activation of a HyperCoal to develop activated carbons for electric double-layer capacitors," *Analytical and Applied Pyrolysis*, vol. 105, pp. 116-121, 2014.

[82] R. L. Tseng and S. K. Tseng, "Pore structure and adsorption performance of the KOH-activated carbons prepared from corncob," *Journal of Colloid and Interface Sscience,* vol. 287, no. 2, pp. 428-437, 2005.

[83] C. Sook Fong, *Fabrication of Porous Gallium Nitride by Photoelectrochemical Etching Method*, Malaysia: Penerbit Universiti Sains Malaysia, 2017, pp. 178-203.

[84] G. P. Wu, C. X. Lu, L. C. Ling and Y. G. Lu, "Comparative investigation on the thermal degradation and stabilization of carbon fiber precursors," *Polymer Bulletin,* vol. 62, no. 5, pp. 667-678, 2009.

[85] S. Arbab and A. Zeinolebadi, "A procedure for precise determination of thermal stabilization reactions in carbon fiber precursors," *Polymer Degradation and Stability*, vol. 98, no. 12, pp. 2537-2545, 2013.

[86] J. C. Lee, B. H. Lee, B. G. Kim, M. J. Park, D. Y. Lee, I. H. Kuk, H. Chung, H. S. Kang, H. S. Lee and D. H. Ahn, "The effect of carbonization temperature of PAN fiber on the properties of activated carbon fiber composites," *Carbon,* vol. 35, no. 10-11, pp. 1479-1484, 1997.

[87] F. Asaad, b. Hassana and H. Elhadidy, "Production of Activated carbons from waste carpet and its application in methylene blue adsorption: Kinetic and thermodynamic studies," *Journal of Enviromental Chemical Engineering,* vol. 5, pp. 955-963, 2017.

[88] D. Xinhuni, C. Srinivasakannan, W. Xin, W. Fei and L. Xinyi, "Synthesis of activated carbon fibers from cotton by microwave induced H3PO4 activation," *Journal of the Taiwan Institute of Chemical Engineering,* vol. 70, pp. 374-381, 2017.

[89] O. Abdelwahab and N. K. Amin, "Adsorption of Phenol From Aqueous Solutions by Luffa Cylindrica Fibers:kinetics,Isotherm and Thermodynamic Studies," *The Egyptian Journal of Aquatic Research,* vol. 39, no. 4, pp. 215-223, 2013.

[90] K. K. Beltrame, A. L. Cazetta, P. C. de Souza, L. Spessato, T. L. Silva and V. de Cinque, "Adsorption of caffeine on mesoporous activated carbon fibers prepared from pineapple plant," *Ecotoxicology and Environmental Safety,* vol. 147, pp. 64-71, 2017.

[91] T. Ibrahim, M. A. Sabri, M. I. Khamis, Y. A. Elsayed, Z. Sara and B. Hafez, "Produced water treatment using olive leaves, Desalination and Water Treatment," *Desalination and Water Treatment,* vol. 60, pp. 129-136, 2017.

[92] K. Y. Foo and B. H. Hameed, "Insights into the modeling of adsorption isotherm systems," *Chemical Engineering Journal,* vol. 156, pp. 2-10, 2010.

[93] Y. S. Ho, "Review of second-order models for adsorption systems," *Journal of hazardous materials*, vol. 136, no. 3, pp. 681-689, August 2006.

Appendix A

A.1 TGA graphs

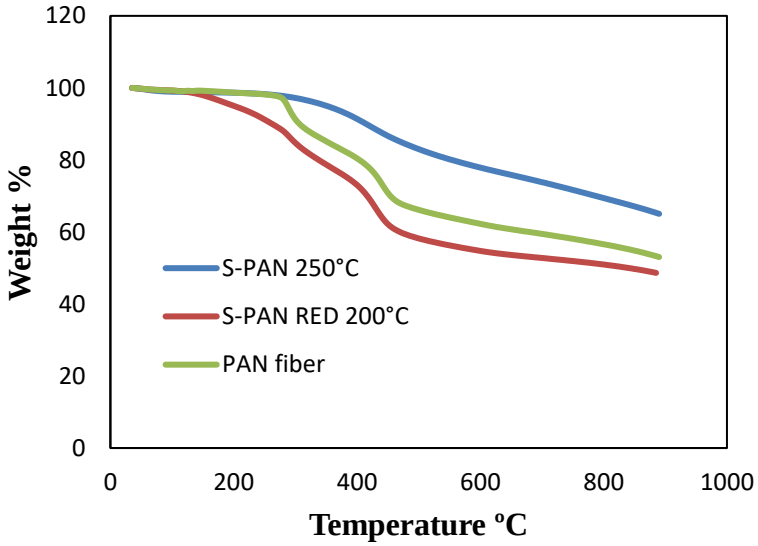

Figure 26: Thermo-gravimetric curves representing the percentage (%) weight loss for stabilized 250°C, stabilized 200°C, and PAN fibers.

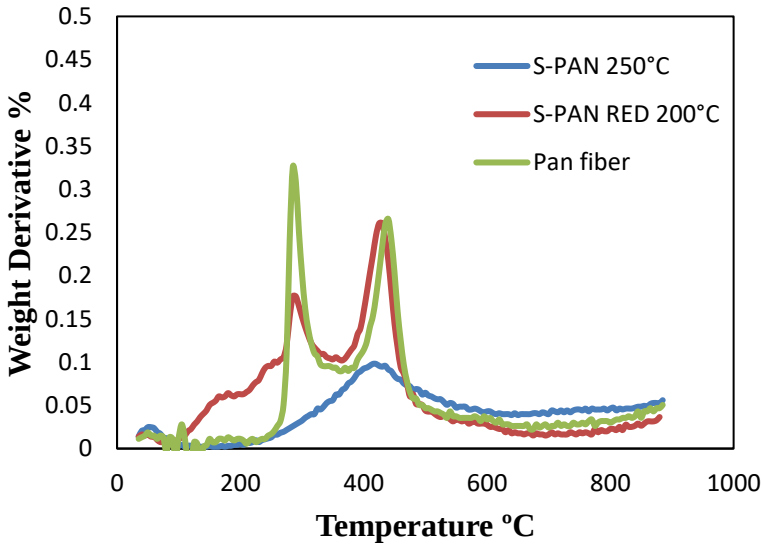

Figure 27: Differential thermo-gravimetric curves representing the derivative weight percentage (%) of stabilized 250°C, stabilized 200°C, and PAN fiber.

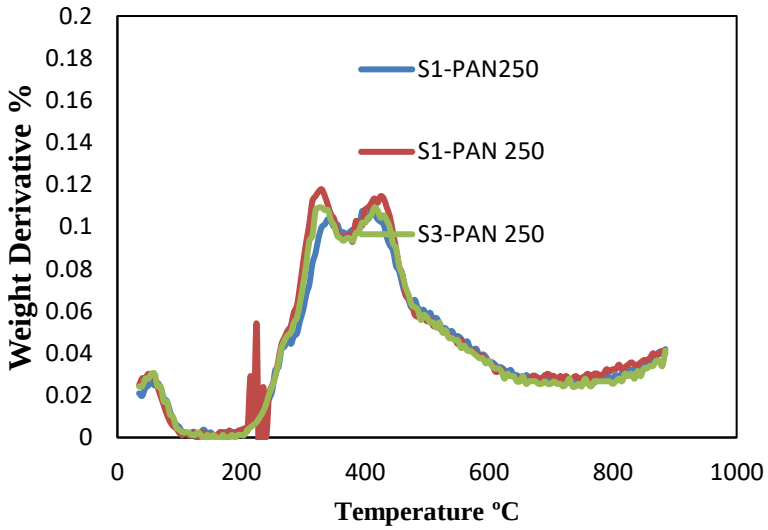

Figure 28: Thermo-gravimetric curves representing the percentage (%) weight loss for stabilized fibers under same condition for different runs.

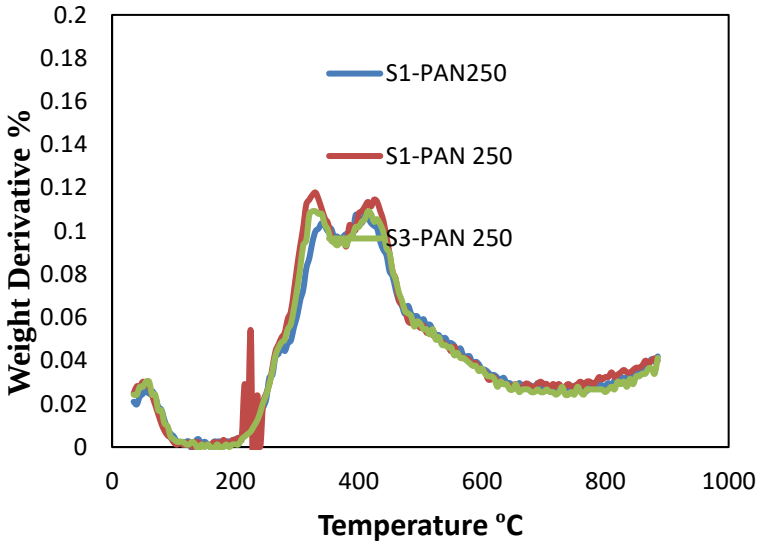

Figure 29: Differential thermo-gravimetric curves representing the derivative weight percentage (%) for stabilized fibers under same condition for different runs.

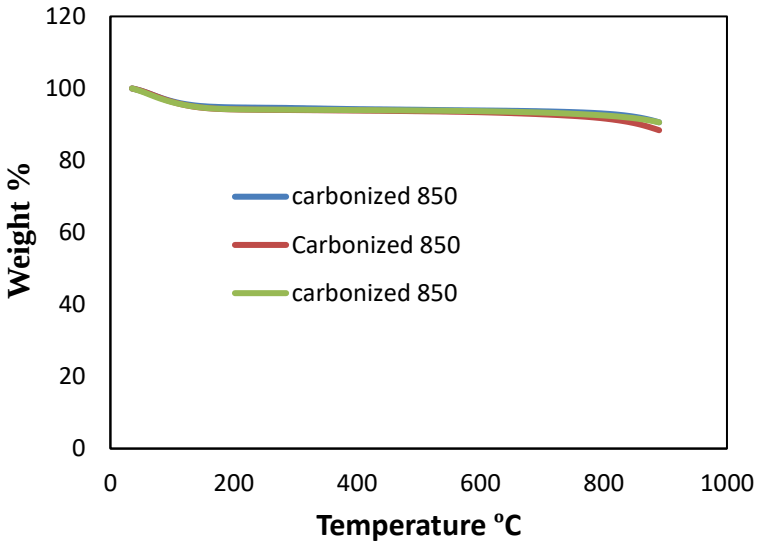

Figure 30: Thermo-gravimetric curves representing the percentage (%) weight loss for carbonized fibers under same condition, temperature = 850°C, time = 2 hours for different runs.

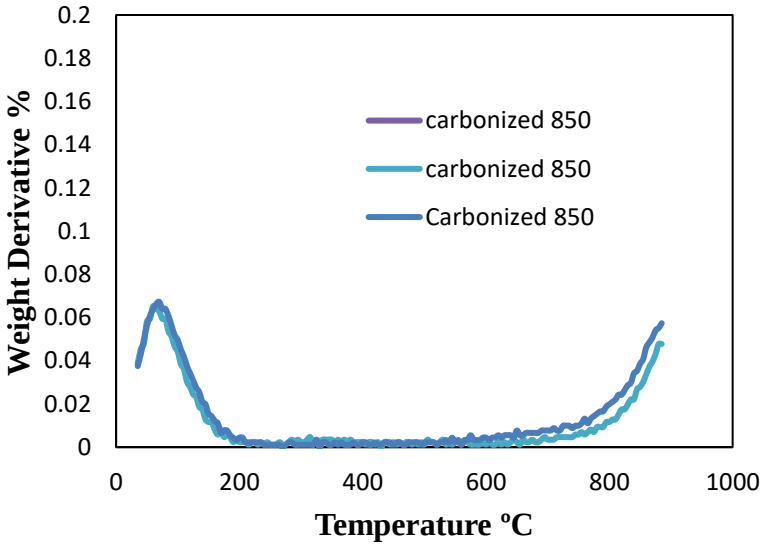

Figure 31: Differential thermo-gravimetric curves representing the derivative weight percentage (%) carbonized fibers under same condition, temperature = 850°C, time = 2 hours for different runs.

A.2 Sample of Adsorption Calculation

Table 12: Optimum dosage calculation Syn-ACFs (KOH).

Dosage	Run	Absorbance	Concentration	Removal Efficiency %
2	1	0.0912	6.706	98.10
	2	0.0861159589	6.332	
	3	0.096165958	7.071026324	
1.5	1	0.1820	13.38298816	96.59
	2	0.1374	10.107	
	3	0.1675	12.314	
1	1	0.4770	35.070	90.18
	2	0.4668	34.324	
	3	0.4574	33.633	
0.6	1	0.1949	143.27	65.71
	2	0.1893	139.21	
	3	0.1923	141.40	
0.5	1	0.1622	119.28	60.76
	2	0.2190	160.99	
	3	0.1790	131.27	

Final concentration with no dilution:

$$\frac{Absorbance}{slope\ of\ calibration\ curve} = \frac{0.0921}{0.0136} = 6.706$$

Removal Efficiency% by ACFs

$$= \frac{initial\ concentration\ of\ (p-cresol) - final\ concnetration}{Initial\ concentration\ of\ (p-cresol)} * 100 =$$

$$\frac{350 - 6.706}{350} * 100 = 98.10\%$$

At 0.5 and 0.6 adsorbent dosage *10 dilution was required to find the removal efficiency %.

Table 13: Optimum parameters of removal of cresol using Syn-ACFs.

Parameters studied	**Optimum value**
Syn-ACFs dosage	1.00 g/L
Contact time	30 minutes
Initial pH	4.6
Temperature	25 C

A.3 Tables for isotherms and kinetics of p-cresol.

Table 14: Values used in isotherm models.

C_i (ppm)	**C_e (ppm)**	**q_e ($\frac{mg}{g}$)**	**C_e/q_e ($\frac{L}{g}$)**	**R_L**
116.49	7.28	109.2	0.067	0.001
310.1	26.9	283.2	0.095	0.001
435.6	68.9	366.7	0.19	0.000
526.2	110.2	415.9	0.27	0.000

Table 15: Values used in kinetic models.

C_i (ppm)	350				
Dosage(g/l)	1				
Time (minutes)	**C_e (ppm)**	**q_e** ($\frac{mg}{g}$)	**q_t** ($\frac{mg}{g}$)	**ln (q_e-q_t)**	**t/qt** ($\frac{g.mins}{mg}$)
5	78.1	335.7	291.9	3.78	0.01
10	57.8	335.7	312.2	3.16	0.03
20	49.4	335.7	320.6	2.71	0.06
30	41.7	335.7	328.3	2.00	0.09
60	34.3	335.7	335.7	-	0.18
90	39.1	335.7	330.9	1.55	0.27
120	39.8	335.7	330.2	1.70	0.36

A.4 SEM images

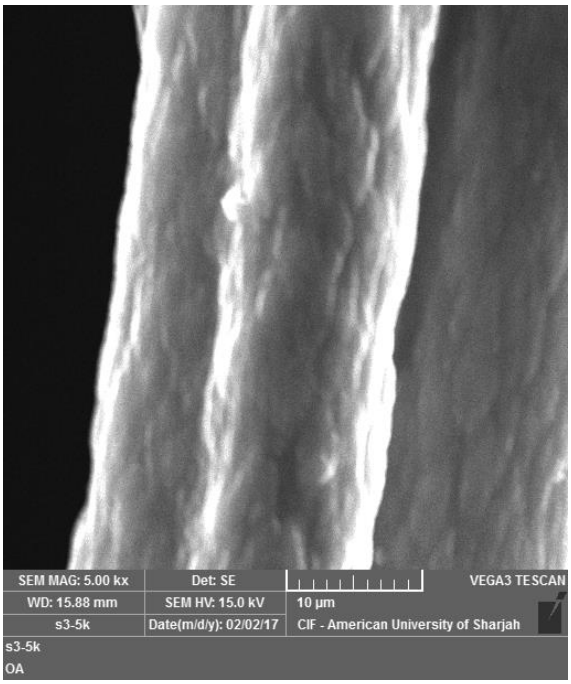

Figure 32: SEM images of Carbonized PAN fibers at 950˚C

Vita

Doaa Salim Samhan Alkathiri was born in 1992, in Salalah, Sultanate of Oman. She graduated from high school in 2010 from Dubai National School. She received her Bachelor's degree in Chemical Engineering from the American University of Sharjah and graduated in spring 2015. In fall 2015, she joined the Chemical Engineering master's program at American University of Sharjah.